

Tsunami and seiche-triggered deformation within offshore sediments

G. Ian Alsop ^{a,*}, Shmuel Marco ^b

^a Department of Geology and Petroleum Geology, School of Geosciences, University of Aberdeen, Aberdeen, AB24 3UE, UK

^b Department of Geophysics and Planetary Sciences, Tel Aviv University, Tel Aviv 69978, Israel

ARTICLE INFO

Article history:

Received 21 December 2011

Received in revised form 8 March 2012

Accepted 10 March 2012

Available online 20 March 2012

Editor: J. Knight

Keywords:

Seiche

Tsunami

Soft sediment

Folding

Slump

Dead Sea Basin

ABSTRACT

Most studies of tsunami and seiche related deposits have focussed on coastal and near coastal zones which are most readily accessible, with few investigations of deeper water settings and the potential soft-sediment deformation effects of such waves. The Late Pleistocene Lisan Formation outcropping to the west of the Dead Sea contains superb examples of sedimentary slump folds formed in water depths of <100 m. We have collected new structural data from an individual horizon that demonstrate that these gravity-driven slumps may be coaxially refolded and reworked by sheared folds and thrusts verging both back up and then down the palaeoslope. This suggests that it is possible to generate upslope flow of material in some circumstances. A progressive increase in reworking and shearing is developed up through the folded sediment, culminating in a breccia layer that is capped by a thin, typically graded horizon of undeformed silt and sand. We suggest that these sequentially reworked deposits are consistent with seismically triggered tsunami and seiche waves that would flow back and forth across the main slump horizon triggered by the same earthquake. The overlying sands and silts that infill local topography are considered to be deposited from turbid suspension during cessation of wave action and represent homogenite deposits. Although tsunami and seiche waves have previously been both numerically modelled and directly witnessed in the Dead Sea Basin, this study forms the first detailed structural analysis and interpretation of potential reworking associated with such waves in offshore settings, where the potential for preservation in the geological record is increased.

© 2012 Elsevier B.V. All rights reserved.

1. Introduction

Tsunamis within enclosed lakes are typically referred to as the initial wave produced by displacement normally triggered by an earthquake, and a seiche is the harmonic resonance of waves within the lake as the water then “sloshes” back and forth (e.g. Ichinose et al., 2000). Most studies of tsunamis have concentrated on the coastal and near coastal zones which are most readily accessible, with few investigations of deeper water settings and the potential soft-sediment deformation effects of tsunami waves (Bryant, 2001). Much research has focussed on the sedimentology and deposition of sand units and associated coarser deposits in this coastal environment, together with their possible subsequent erosion by backwash or later tsunami waves. However, not all tsunamis leave coarse deposits in shallow marine environments, as this depends on their intensity (e.g. Noda et al., 2007) and the availability of sediment.

The inundation (or wave) height at the shore is broadly equivalent to the vertical offset of the sea floor, and this empirical relationship suggests that tsunami deposits around oceans require earthquakes of magnitude 8 or greater (Dawson and Stewart, 2007). In general, a minimum

tsunami inundation height of 5 m along the shore is considered necessary to leave a recognisable deposit on the onshore record (Lowe and de Lange, 2000; Dawson and Stewart, 2007). Dawson and Shi (2000) note however that the deposition and preservation of any tsunami deposit is dependent principally upon an adequate supply of sediment, and that near shore zones with little sediment make it possible for a tsunami to strike a coastline but leave no trace of its passage (Dawson and Stewart, 2007). In addition, sediment deposition may take place entirely above the mean sea level during the tsunami surge (Morton et al., 2007) and hence leave little evidence in the deeper water setting. Therefore the offshore, deeper water erosional and depositional signature of tsunamis may be very different to the frequently studied coastal and onshore deposits. The difficulty in separating possible deeper water tsunami deposits and structures from those associated with turbidity and debris flow sequences has been highlighted recently by Dawson and Stewart (2007). However, the possibility of recognising deeper water tsunami deposits is useful due to their greater preservation potential in the geological record when compared to beach and near-shore environments.

Descriptions of sediment folding and faulting generated by seiche and tsunami waves are uncommon, although they have been recently recorded from muddy siltstones interpreted to be deposited from a Precambrian tsunami affecting a back shore facies exposed in Central India (Sarkar et al., 2011). This deformation is considered to relate to sediment slumping caused by the outgoing or backwash component

* Corresponding author.

E-mail address: Ian.Alsop@abdn.ac.uk (G.I. Alsop).

of tsunami flow. It results in ~10 cm scale folds verging and overturning towards the offshore direction, ultimately creating recumbent folds in argillaceous sediments deposited from the tsunami itself (Sarkar et al., 2011). Axial planes of these downslope verging folds dip towards the on shore, and the whole fold system is considered to ride on an underlying detachment or shear plane (Sarkar et al., 2011 p. 186). These authors suggest that slumping, marked by folding and faulting, was created by a significant backwash event in the back shore zone created by tsunami retreat. Observations in Holocene sediment cores from lakes in the Alps that were interpreted as evidence of seiche-triggered deformation include homogenites, liquefaction and flowage, and micro-fracturing (Beck, 2009). Older (Miocene) lacustrine deposits from the Betic Cordillera of southern Spain were interpreted as seismites based on graded deformation showing similar structure as the Lisan seismites. They are interpreted as the result of an oscillating sense of shear at the water-lakebed interface (Rodríguez-Pascua et al., 2003). Moretti et al. (2001) identify asymmetric folds in lacustrine beds as deformation related to two driving forces: unstable density gradient and lateral shear stress induced by the downslope component of the sediment weight.

In order to address and discuss some of the problems associated with possible deformation of sediments by seiche and tsunami waves in the offshore environment, we provide a detailed case study from the Late Pleistocene (70–15 ka) Lisan Formation deposited in the precursor to the Dead Sea. The Dead Sea Basin is an ideal place to study the offshore effects of seiche and tsunami waves due to regional tectonic activity coupled with the enclosed nature of the basin, that will naturally encourage seiche and tsunami (or “harbour”) waves to develop. Our study aims to explore a number of factors and fundamental questions pertaining to deformation of unlithified sediments. This includes the analysis of folds that verge back up and then down the regional slope, culminating in breccias that are capped by graded clastic units. We assess a range of possible scenarios for the generation of such structures including the likely effects that tsunami or seiche events may have on slump fold patterns in deeper water (~100 m) conditions. To provide a general background, we first present a brief overview of soft sediment folding associated with slumping in unlithified sediments.

2. Soft sediment folding

Folding is typically considered the most obvious of structures associated with deformation of poorly-consolidated sediments (e.g. Woodcock, 1976a, 1976b, 1979; Maltman, 1984, 1994a, 1994b;

Elliot and Williams, 1988; Collinson, 1994). A general increase in pore fluid pressure is known to dramatically reduce the shear strength of sediments and thereby facilitate such soft-sediment deformation (e.g. Maltman, 1994a, 1994b and references therein). A number of mechanisms, including seismicity, may result in local increases in pore fluid pressure, and hence trigger slumping (e.g. see Alsop and Marco, 2011). However, resulting folding is intuitively thought to be linked to gravity-driven slump processes along a basal detachment, with the expectation that fold geometries will reflect the palaeoslope upon which they were created (Farrell and Eaton, 1987, 1988; Martinsen, 1989; Martinsen and Bakken, 1990; Bradley and Hanson, 1998; Debacker et al., 2001, 2006; see review in Alsop and Marco, 2012) (Fig. 1). Detailed examination of slump-related deformation reveals both contractional folding and extensional faulting that may display a range of orientations and geometries reflecting possible deformation cell scenarios (see Alsop and Holdsworth, 2007; Debacker et al., 2009; Alsop and Marco, 2011). However, the over-riding consideration is that folds and faults will display vergence patterns that broadly define the downslope slump direction (Fig. 1).

Fold facing is defined as the direction along the axial surface, and normal to the fold hinge, in which younger rocks are encountered (see Holdsworth, 1988; Alsop and Marco, 2011, 2012 for further details). The facing direction is upwards and parallel to the direction of flow in situations where fold hinges form broadly normal to transport and undergo little or no subsequent rotation (Fig. 1). Where fold hinges have suffered later rotation during progressive shearing to create curvilinear sheath fold geometries, then facing attitudes will typically become sub-horizontal and define a range of directions reflecting the arc of hinge orientations (e.g. Alsop and Holdsworth, 2004a, 2004b; Alsop et al., 2007) (Fig. 1). Differential shear within slumped masses may encourage folds to initiate (and hence face) at a range of angles to the slope direction (Alsop and Holdsworth, 2007), although this does not appear to be the case in the Dead Sea examples (Alsop and Marco, 2011, 2012).

The critical factor in gravity-driven soft-sediment deformation is that both fold vergence and associated facing directions will form parallel to, or define an arc about, the direction of downslope slump transport (see Alsop and Holdsworth, 2002, 2004b, 2007; Strachan and Alsop, 2006; Alsop and Marco, 2011, 2012) (Fig. 1). The recognition in this study that distinct horizons of folds define an opposing sense of vergence and facing to the established downslope direction therefore leads us to pay particular attention to the genesis of such horizons and their role in the deformation process.

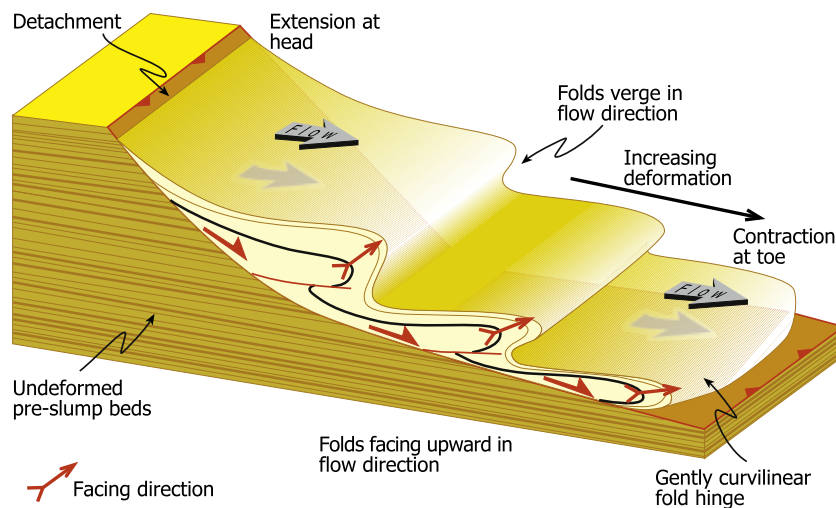


Fig. 1. Schematic cartoon illustrating a typical slump-related fold and fault system over riding undeformed horizontal pre-slump beds. The slumped mass translates downslope along a basal detachment and is marked by extension at the (upper) head of the slump and contraction associated with folds and thrusts at the toe. Folds progressively tighten with increasing deformation down the slump system, whilst their axial planes and associated facing directions sequentially rotate and flatten, ultimately resulting in recumbent curvilinear fold hinges.

3. Geological setting of the Dead Sea case study

The Dead Sea Basin is a pull-apart structure on the Dead Sea transform, which is marked by two major parallel fault strands that generate numerous earthquakes (e.g. Marco et al., 1996, 2003; Ken-Tor et al., 2001; Migowski et al., 2004; Begin et al., 2005) (Fig. 2a, b). This transform is thought to have been active from the Miocene to recent, including during deposition of the Late Pleistocene (70–15 ka) Lisan Formation that forms the focus of the present study (e.g. Bartov et al., 1980; Garfunkel, 1981 Haase-Schramm et al., 2004).

The Lisan Formation comprises a sequence of finely laminated annual varve-like repetitions of aragonite and clastic rich couplets considered to represent dry summers and winter flood events respectively (Begin et al., 1974). Although deposited on slopes of $<1^\circ$, the Lisan Formation contains numerous intraformational fold and thrust horizons that are capped by undeformed beds and are considered to be seismically triggered (Alsop and Marco, 2011). The formation is exposed for ~100 km along the western shore of the Dead Sea and displays systematic variation in the orientation of slump fold and thrust systems within it. In the northern portions around Jericho slumping is directed towards the SE, in the central portion around En Gedi and Masada slumping is towards the east, whilst in the southern area around Peratzim slumping is NE-directed (Alsop and Marco, 2012) (Fig. 2c). Combined with westerly-directed slump folds recorded from the eastern shore of the Dead Sea in Jordan (El-Isa and Mustafa, 1986), this suggests a regional pattern of radial slumping towards the depocentre of the Dead Sea Basin (Alsop and Marco, 2012).

The Dead Sea Basin is an ideal place to study structures associated with seiche/tsunami in offshore environments as it is a well defined and restricted basin containing the major Dead Sea Fault noted above (Fig. 2b). There is a long and detailed seismic record resulting from movement on these faults, with displacement of the sea floor demonstrated by sedimentary growth strata around faults, and also suggested by release of bitumen after major earthquakes. The hypersaline Dead Sea also provides a detailed chemical record of mixing of the entire water column in deeper water settings, that will typically be absent in less saline basins. The relatively cohesive muds and precipitated aragonitic layers define an intricate varve-like stratigraphy that define a range of detailed structures that may not survive elsewhere, whilst the lack of bioturbation in the hypersaline water also allows preservation of detail. The relatively enclosed and small size of Lake Lisan and the Dead Sea Basin means that structures generated will always be relatively proximal to earthquakes. In addition, the possible effects of storm waves are likely to be more limited as they do not have a long fetch to develop large amplitudes, whilst tidal currents will also be negligible due to the limited size of the basin.

The slump horizons and reworked zones of sediment we are particularly interested in for this case study are best exposed in the Peratzim Creek in the southern Dead Sea (see Alsop and Marco, 2011) (Fig. 2c, d). We focus on an individual 1.5 m thick deformed horizon at N31°0449.6 E35°2104.2 that may be confidently traced across strike for 250 m before exposure terminates. Peratzim is positioned 1 km east of the bounding Dead Sea Fault, with Cenomanian carbonates preserved further to the west in the footwall to this fault. For most of the time between 70 and 28 k, Lake Lisan at Peratzim had a maximum depth of 100 m or less, apart from a brief period from 26 to 24 ka when water was up to 200 m deep (Bartov et al., 2003). Cross laminations are locally observed in the lower parts of the Lisan Formation and adjacent to a coarser facies interpreted as shoreline beach deposits exposed further to the west. However, their absence higher in the Lisan Formation in the case study area suggests an absence of physical processes such as storm waves and indicates that water depths therefore exceeded 30 m (Noda et al., 2007). It is likely therefore that water depths were somewhere in

the range of 30–100 m for much of the deposition and associated deformation of the Lisan Formation at Peratzim.

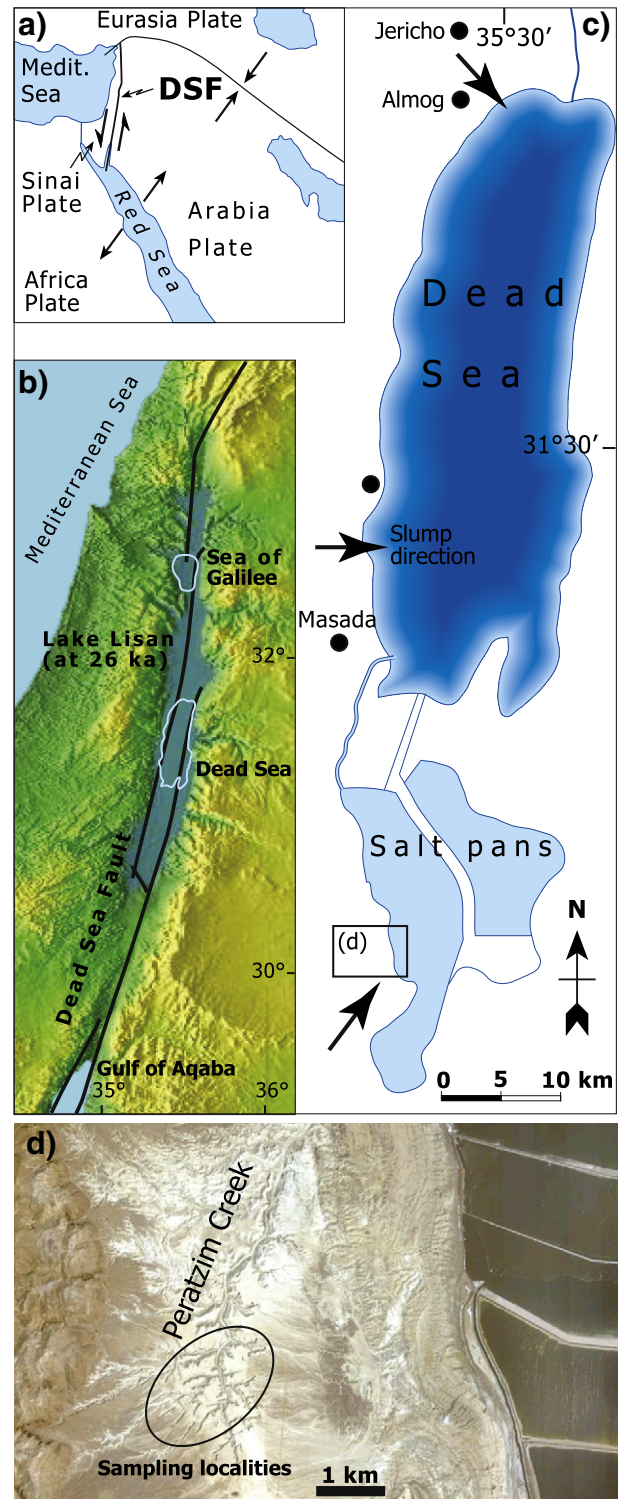


Fig. 2. a) Tectonic plates in the Middle East. General tectonic map showing the location of the present Dead Sea Fault (DSF). The Dead Sea Fault transfers the opening motion in the Red Sea to the Taurus–Zagros collision zone. b) Generalised map showing the maximum extent of Lake Lisan along the Dead Sea Fault at 26 ka. c) Map of the current Dead Sea showing the position of localities referred to in the text. Arrows indicate mean direction of slump transport from Alsop and Marco (2012). d) Google Earth image of the Peratzim Creek study area. Circle marks the data collection points.

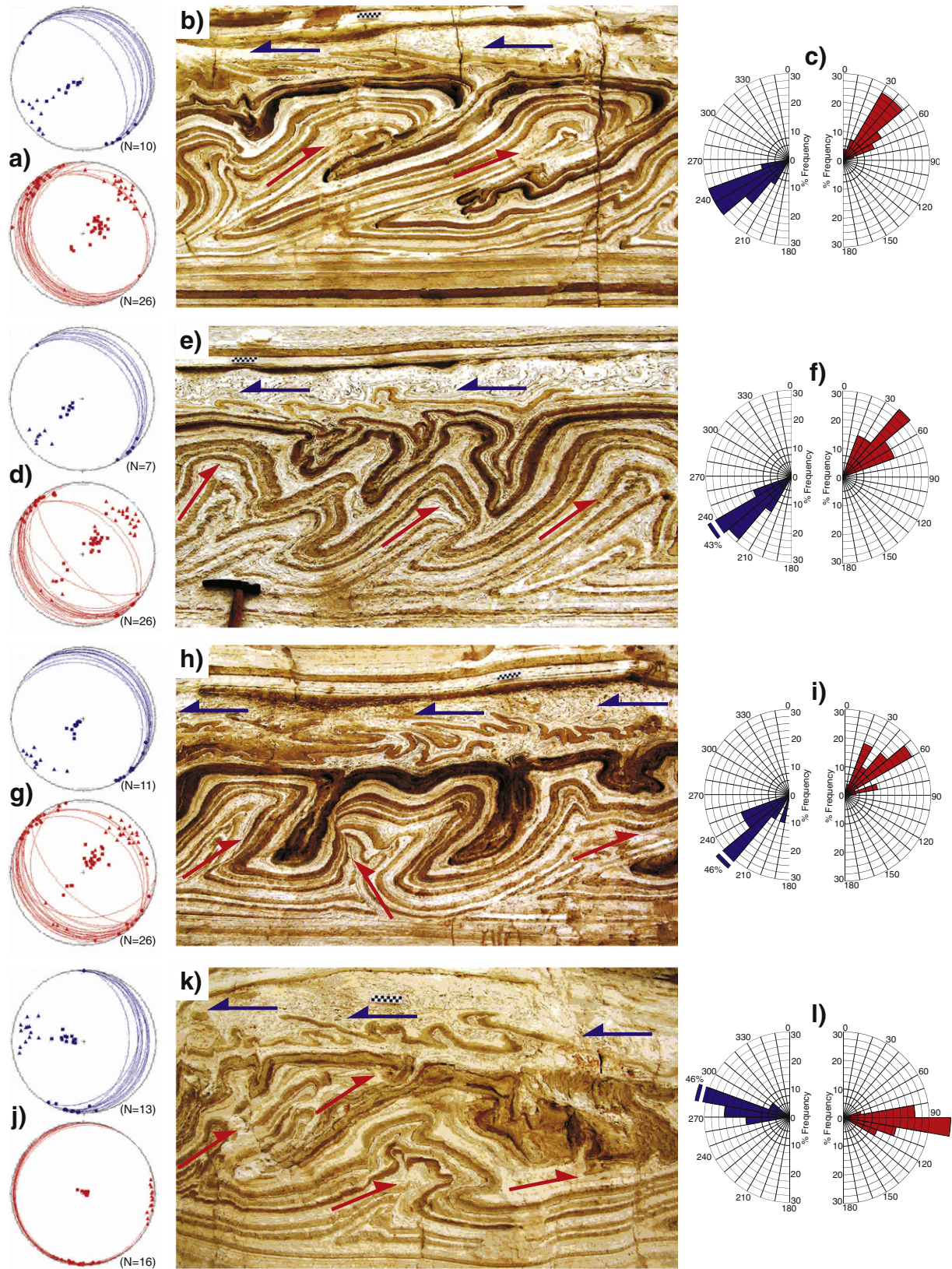


Fig. 3. Sets of stereonets (a, d, g, j), photographs (b, e, h, k) and rose diagrams (c, f, i, l) from the case study horizon at Peratzim. The photographs show the NE-verging slump overlain by SW-verging structures and breccia. Scale is shown by a 10 cm long chequered ruler or 30 cm hammer. Equal area stereoplots show fold hinges (circles) and axial surfaces displayed as both great circles and squares representing poles. Upward facing directions are plotted as solid triangles which are projected vertically down (as chordal points) from their upper hemisphere intersection onto the lower hemisphere stereonet. In each pairing, NE-verging slump fold data is shown in the lower (red) stereonet whilst overlying SW-verging folds are shown on the upper (blue) stereonet. Facing directions are also highlighted on the associated rose diagrams, with NE-facing folds on the right (red) and SW-facing on the left (blue) in each case.

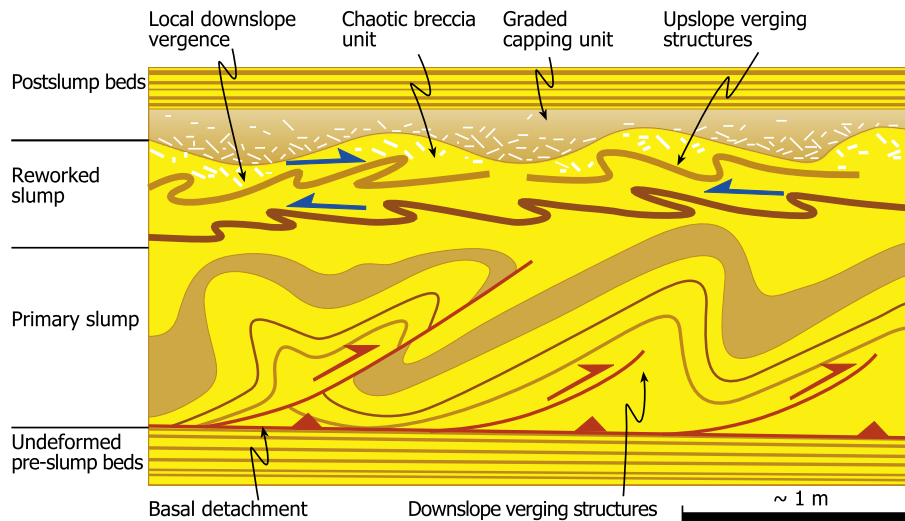


Fig. 4. Summary schematic section illustrating the geometry of primary downslope verging folds and thrusts (shown in red) overlain by a zone of upslope vergence and reworking (highlighted by blue arrows). The intensity of deformation increases up through the reworked zone, and is associated with reversals in vergence culminating in a chaotic breccia unit. The deformed sequence is truncated by overlying post slump beds marked by an irregular erosive base and a graded capping unit.

4. Observations of fold and fabric relationships through the deformed horizon

Having established that the Lisan Formation displays a large-scale radial slump pattern towards the Dead Sea Basin (Alsop and Marco, 2012), we now describe detailed observations from an individual slumped horizon at Peratzim that displays reworking of these structures. It is important to note that all of these units are cut by sedimentary injections confirming the syn-sedimentary nature of the deformation (see Marco et al. 2002; Alsop and Marco, 2011). The poorly lithified nature of the sediment allows careful excavation of structures to determine 3D geometry, although their weakness does not facilitate thin section sampling. All photographs are orientated with NE towards the right, with red arrows highlighting NE-directed slumping whilst blue arrows relate to overlying zones of reworking. Photographic scales are shown either by a 15 mm diameter coin, 10 cm long chequered ruler or 30 cm hammer.

4.1. Observations of primary slumping and downslope verging structures

Undeformed (pre slump) horizons are parallel bedded, dip towards the east at angles of $<1^\circ$ and are typically separated from overlying slumped units by a basal detachment that forms a structural decollement upon which downslope directed translation has occurred (Figs. 3, 4). The basal detachment to the slump system is largely parallel to the cm-scale laminated bedding surfaces of the Lisan Formation. The depth of this detachment at the time of slumping is a minimum of 1.5 m, with some overlying material having been lost through subsequent erosive action, whilst the dip of the basal detachment at the time of slumping is less than 1° (see Alsop & Marco 2011, 2012). Folds within this primary slump unit are typically <1 m wavelength and form a deformed horizon that is <1.5 m thick (Fig. 3b, e, h, k). Fold attitude varies between upright to recumbent with typically rounded hinges. Folds are typically NW–SE trending (Fig. 3a, d, g, j) with uniform orientations suggesting a lack of markedly curvilinear folds and only limited hinge rotation during slumping. Associated

axial surfaces dip gently-moderately towards the SW, although NE-dipping axial surfaces are locally developed and relate to minor back folds. Poles to axial surfaces therefore define a broadly bimodal pattern forming a partial girdle (Fig. 3a, d, g, j). Facing directions are towards the NE (046°) (Fig. 3c, f, i), although this may locally deviate towards the east in adjacent sections (Fig. 3j, k, l).

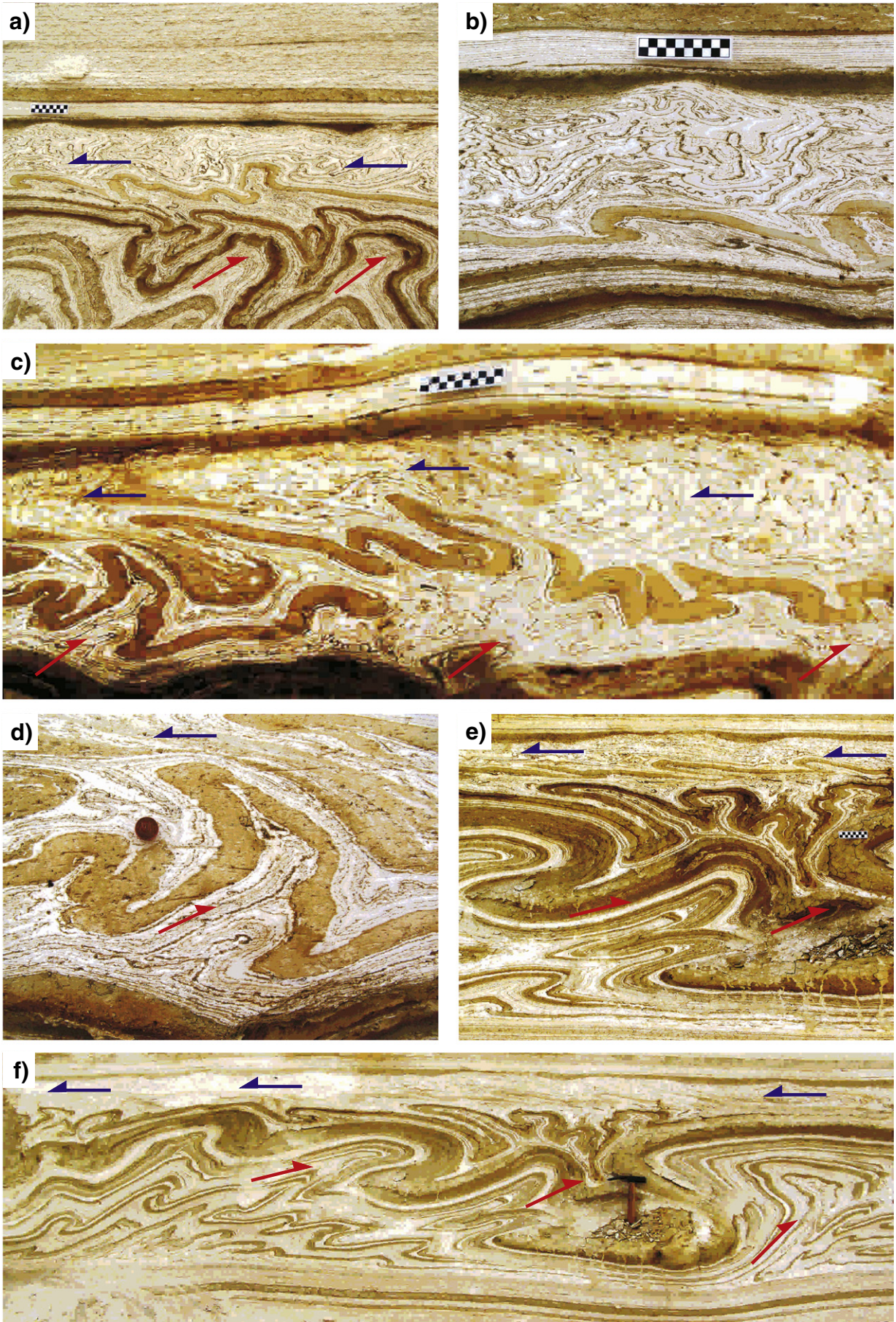
Overall, the downslope verging folds and thrusts form exceptionally coherent and ordered systems typically related to sequential thrusting and folding in a basin-ward propagating piggyback sequence (see Alsop and Marco, 2011) (Fig. 4). Within the slumped horizon, there is no evidence for multiple or punctuated phases of NE-directed movement. Folds and fabrics may however be sequentially reworked during a single progressive NE-directed deformation, resulting in continuous re-fold patterns (Alsop and Marco, 2011).

4.2. Observations of reworking and upslope verging structures

The upper portions of the downslope verging primary fold and thrust system described above are reworked and overlain by younger structures (Figs. 4, 5a–f, 6a–g, 7a–h, 8a–h). These overlying folds are typically NW–SE trending (140°) (Fig. 3a, d, g, j) with uniform orientations. Associated axial surfaces dip consistently gently towards the NE, with poles to axial surfaces therefore defining a clustered pattern. Fold facing directions are towards the SW (230°) (Fig. 3c, f, i), although this may locally deviate towards the west in adjacent sections (Fig. 3j, k, l). A reversal in facing polarity therefore exists between the underlying NE-directed slump system and the overlying SW-verging folds. In detail, the facing directions are not diametrically opposed, with the mean overlying SW-directed folds developed consistently clockwise (-4°) of the diametric opposite to the NE slumps (Fig. 3, c, f, i, l).

The overlying folds have wavelengths <30 cm and are formed in a unit that is typically 20–30 cm thick (Fig. 5a, b, c). Fold attitudes are typically overturned to recumbent, with tight-isoclinal interlimb angles and rounded to angular hinges (Fig. 5a, b, c). Darker clastic-rich

Fig. 5. Photographs of SW-verging folds and breccia with scale shown by a 10 cm long chequered ruler, 30 cm hammer or 15 mm diameter coin. a) NE-verging slump folds in the lower part of the section reworked by SW-verging structures. b) Details of folds and overlying capping sediment from the left side of a). Refer to Fig. 3e for location. c) SW-verging folds displaying increasing deformation up through the sequence. The deformed unit is capped by a (dark) clastic bed (with aragonite fragments) immediately below the scale. d) Details of refolding from the left side of c). Originally NE verging folds are reworked by SW-directed shear to create Type 3 refolds. Refer to Fig. 3h. e) NE-verging folds and thrusts overlain by isoclinal SW-verging folds. The later SW-verging folds are moulded round the larger NE-verging structures. The deformed sequence is capped by a dark clastic layer that infills local topography. f) Complete section showing location of e) by hammer. Note imbrications in core of fold (to left) and lateral persistence of thin capping clastic unit.



layers are 1–2 cm thick and define sub-parallel fold shapes (Fig. 5a, b). This indicates that these marker horizons are more competent than the surrounding aragonite-rich unit that contains only thin (mm-scale) clastic laminae. Although marker layers are locally thickened in fold hinges, they can display thinning and extreme attenuation on both the lower limb and upper limbs (Fig. 5c).

In some circumstances classic Type 3 re-fold patterns (e.g. Ramsay, 1967) are created where NE-verging folds are reworked by overlying SW-verging structures resulting in originally SW-dipping axial surfaces being reorientated into NE dips (Fig. 5c, d). This provides a clear temporal constraint with underlying NE-directed structures developed prior to the overlying SW-verging folds. These re-fold patterns are only created towards the base of this reworked unit. Small upslope SW verging folds may be “smeared” around larger NE and downslope verging folds (Fig. 5e, f). This is interpreted as a “moulding” of small folds around larger structures and results in axial surfaces curving around the older downslope verging structures (Fig. 5e, f). It is important to note that the apparent “wrapping” of minor folds around larger NE-verging structures is not therefore considered a consequence of refolding in the classical sense i.e. the NE-verging structures are not regarded as later. Some folds appear to tighten as they are traced upwards, with axial planes rotating into more gently dipping attitudes suggesting an increase in strain (e.g. Alsop and Carreras, 2007). Folds may also be attenuated on their upper limbs due to subsequent flow and increasing shear over the top of the existing fold (Fig. 5d, e, f).

Finally, some SW-verging folds associated with reworking are themselves refolded by overlying NE-verging folds to create hook-shaped interference patterns (Fig. 6a, b). The upper parts of the reworked unit may be marked by sheared bedding, folds, and aligned aragonite fabrics that dip gently towards the SW and also suggest an even later phase of top-to-the-NE shear (Fig. 6c, d, e). In summary, NE-directed slumps are reworked and overlain by a zone of SW-verging fabrics and folds (Fig. 6f). It is also apparent that there are periodic reversals in fold and fabric vergence up through this reworked zone suggesting that the sense of shear also systematically switches up through this unit (Fig. 4 and see below).

4.3. Observations of reworking and the chaotic breccia unit

The increase in deformation up through the folded unit noted above may ultimately result in disaggregation and brecciation of the reworked unit (Figs. 4, 6g, 7a, b). Breccia may be transitional to underlying folds, with some breccia fragments are up to 5 cm long, and containing pre-incorporation folds (Fig. 7c, d). This indicates that brecciation post-dates folding in such cases. In other cases, aragonite clast alignment defines an oblique fabric within the breccia, that may itself then be folded suggesting that folding was intimately associated with brecciation and continued to develop during and after brecciation (Fig. 7e). Folds within the breccias may verge upslope in an opposing direction to NE-directed downslope slumping. Folds within breccia may be upright with recumbent folds on each margin marked by opposing vergence suggesting possible liquefaction and reworking within the breccia (Fig. 7f). The breccia unit may be overlain by an erosive contact which truncates folds and

fabrics within the breccia and reworked unit, before being capped by an overlying and undeformed capping horizon (Fig. 7e, f, g).

4.4. Observations of post-slump undeformed capping unit

It is notable that the deformed and reworked horizon is directly capped by a 2–10 cm (exceptionally up to 30 cm) dark clastic horizon comprising mud, silt, sand and mm-scale aragonite fragments (Figs. 4, 7, 8). The underlying layers are occasionally interfolded with the clastic unit via SW-verging recumbent folds suggesting upslope directed currents operated during its deposition, although no cross lamination is observed (Figs. 6g, 7h). However, no NE-directed downslope verging structures affect or cut the capping sediments, and therefore this unit is interpreted as being deposited after cessation of downslope slumping. This capping unit more typically has a sharp well defined base (Fig. 7e, f), may also display grading with aragonite fragments concentrated towards the base (Fig. 7e), and may locally thicken and thin to infill underlying slump topography (Fig. 7g). The base of this unit may be transitional with the underlying breccia, or locally it may truncate underlying folds and structures to create a marked cut-offs (Fig. 8a, b, c). Structural restoration of “missing” folded sequences suggests that in some cases a minimum of tens of cm of underlying section may be missing (Fig. 8d).

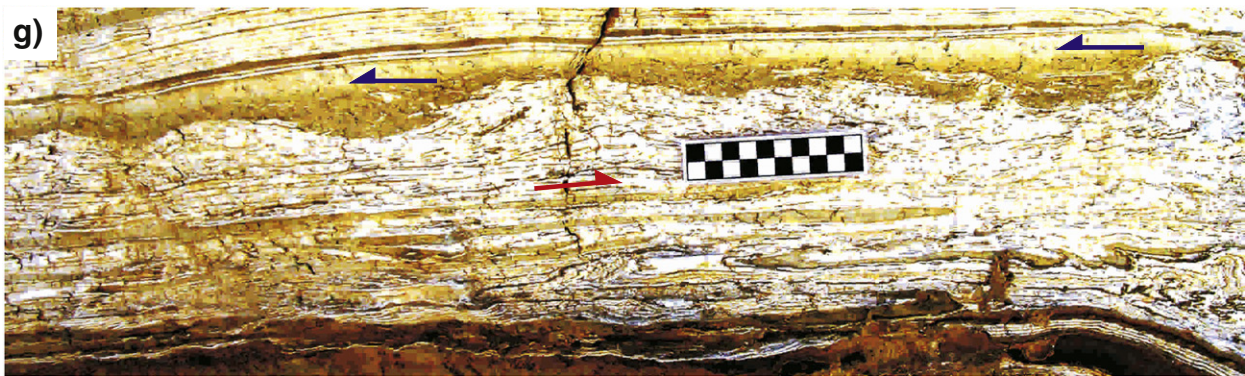
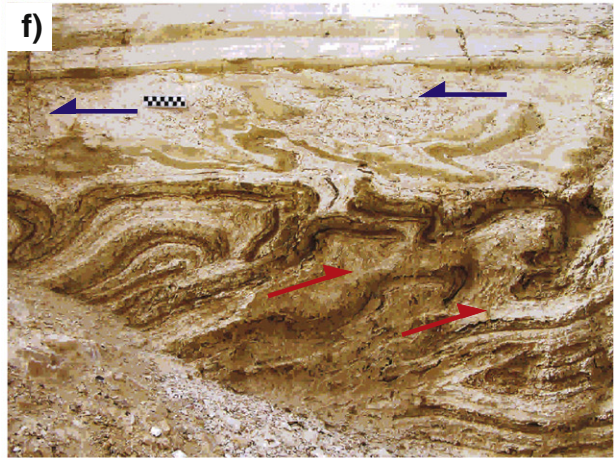
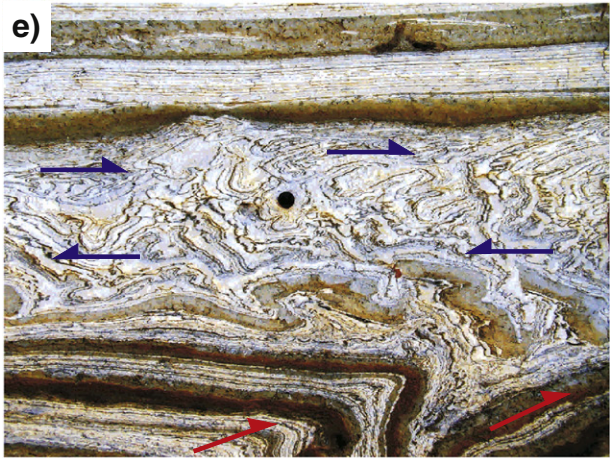
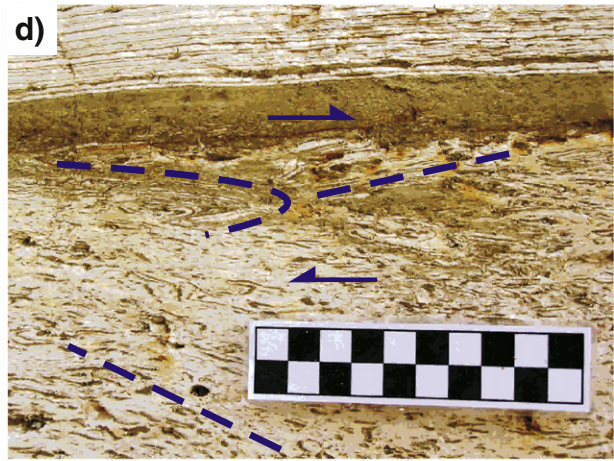
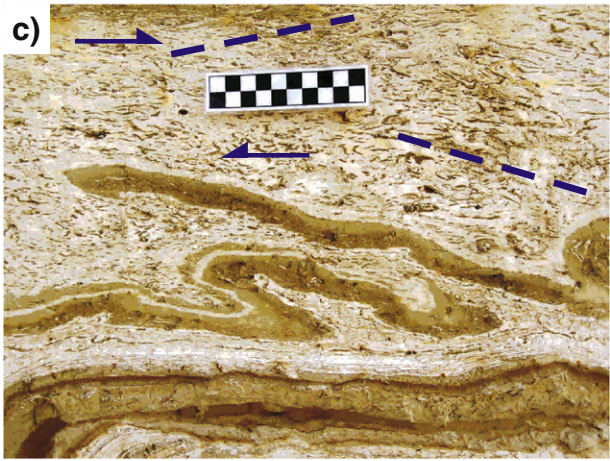
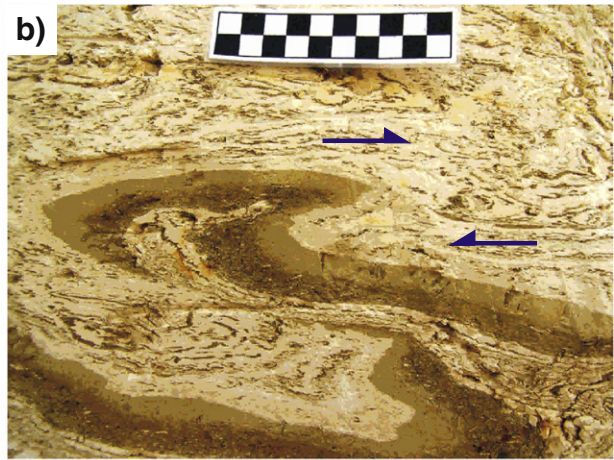
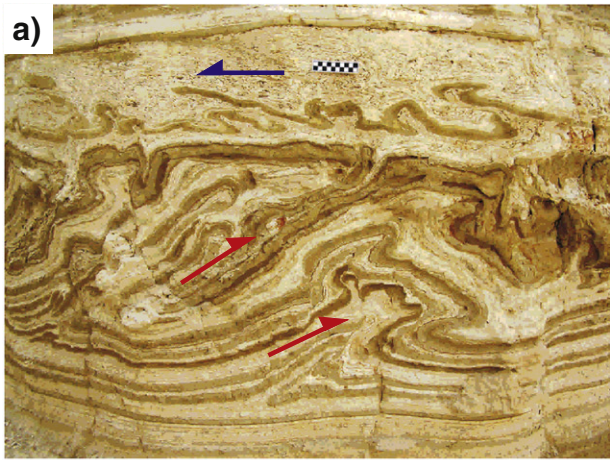
The long axes of aragonite fragments within this capping unit are typically aligned parallel to the underlying surface and follow bathymetry rather than the top surface of the horizon (Fig. 8e). Aragonite fragments remain angular and may be up to a few cm in length although more typically they are on an mm scale. They are considered to be sourced from the underlying sequence. Two distinct layers of aragonite fragments are occasionally observed (Fig. 7e), although a single graded unit is most common. Faint planar laminations are also observed in thicker sequences (Fig. 7g). This clastic unit shows pronounced lateral thickening and thinning to infill topography created by the underlying slump and breccia units (Figs. 7g, 8c, d, e, f). The unit also displays lateral variation in fragments, with layers of fragments frequently concentrated in depositional “lows” on either side of truncated structures (Fig. 8e). Aragonite fragments tend to concentrate on the slightly steeper side of the depositional low, which may represent the lee of ridges in underlying slumped sediments (Figs. 6g, 7g). This lee side is frequently on the SW side, and suggests that this capping unit and associated aragonite fragments were deposited from SW-directed currents. This is in broad agreement with “upslope” shearing of folds noted above and suggests that the overlying clastic unit was not therefore deposited from a downslope flowing current such as may be associated with a turbidite.

In summary, this capping unit is much thicker (up to 30 cm) and quite distinct from the “background” varve-like sedimentation marked by alternations of aragonite- and clastic-rich laminae on an mm scale (Fig. 8g). The top of the clastic unit is horizontal and planar, and parallel to the overlying post-slump beds.

4.5. Summary of critical observations

The following observations and pertinent points have been directly made on the slumped horizon at Peratzim:

Fig. 6. a) Photograph of NE-verging folds overlain by tight SW-directed folding. Deformation intensifies up through the unit and is capped by a thin (dark) clastic horizon. b) Detail from right of the scale in a) showing a SW-verging fold and thrust being refolded by subsequent NE-directed shear to create a hook-shaped re-fold. c) Detail from left of the scale in a) showing SW-directed fold and thrust. d) Details of increasing strain up through the deformed unit culminating in intense folding and brecciation (scale is in same position as b) and refer to a) for location). The brecciated unit is capped by a 2.5 cm thick clastic layer. e) Details of lower NE-verging folds overlain by SW-directed folded and thrust horizon. The upper parts of the reworked zone are marked by NE-verging fabrics (above coin) that display increasing deformation upwards and are capped by a clastic unit of variable thickness. f) General view of NE-verging slump folds overlain by SW-verging structures and capped by an undeformed clastic unit that infills topography. g) NE verging folds overlain by breccia that displays an undulating upper contact with undeformed graded clastic that infills topography. Note that the breccia is intersheared with the clastic unit suggesting a SW sense of mixing and flow. In each case, the scale is shown by a 10 cm long chequered ruler or 15 mm diameter coin.



- (i) The primary slumped unit comprises NE-verging folds and thrusts typically marked by SW-dipping axial planes and which face upwards towards the NE (046°) (Figs. 8g, h, 9a, b). These are developed above a basal detachment and relate to downslope directed slumping towards the NE.
- (ii) The NE-directed primary slump unit may be reworked by overlying SW-verging folds associated with NE-dipping axial planes and which face upwards towards the SW (230°) (Figs. 8g, h, 9b, c). Minor folds become increasingly recumbent up through the reworked slump unit, and relate to upslope directed shearing towards the SW.
- (iii) There is no evidence of an erosive surface developed between NE-directed downslope slumping and SW-directed upslope verging geometries. The upslope SW-verging structures are always developed directly above, and in structural continuity with, the NE-verging primary slump (Fig. 8e, f, g, h). Upslope verging fold hinges are only developed within the top ~30 cm of the deformed sediment package (Figs. 8 e, f, g, h, 9b). Smaller SW-verging folds may become smeared and moulded around larger underlying NE-verging folds (Fig. 8f).
- (iv) The SW (upslope) – verging folds are themselves reworked and refolded in their upper parts resulting in NE (downslope) – closing “hook-shaped” fold interference patterns (Fig. 6b). This provides a direct temporal relationship related to a switching of flow directions.
- (v) The upslope verging structures may be overlain by up to 20 cm of more chaotic sediments and coarse breccia (Fig. 8 e, f). Minor folds are progressively sheared over (in both the upslope and downslope directions) and are ultimately smeared out as they are traced up through the sediment package into the breccia (Fig. 6e). This suggests an apparent increase in shear stress towards the top of the sediment package and the sediment–water interface.
- (vi) The reworked slumps and chaotic breccia are overlain by post slump beds incorporating an undeformed capping unit that infills slump-related topography (locally up to 30 cm thick) (Fig. 8e, f). This unit displays either a gradational or locally erosive base that truncates the underlying deformed unit. It is marked by aragonite fragments that grade upwards and are concentrated on the steeper (typically SW) flanks of erosive hollows, crucially indicating deposition from a SW (i.e. upslope) -directed current. This thick graded unit is sedimentologically distinct from the mm-scale laminae that comprise the varve-like background sedimentation.

5. Interpretation of fold and fabric relationships through the deformed horizon

Folds verging in the opposite sense to the dominant slump direction have been recorded previously by Woodcock (1976b) and Strachan and Alsop (2006) and experimentally produced by Blay et al. (1977). Major slump folds verging towards the NE down the inferred palaeoslope at Peratzim may be directly reworked and overlain by minor folds and thrusts with an opposing (SW-directed) vergence back upslope (e.g. Figs. 9, 10). This reversal in vergence (and inferred flow direction) could be caused by a number of factors that will now be considered.

5.1. A reversal in the structural position of minor folds

Minor folds located on the short, atypical limbs of larger scale folds may display an opposing sense of vergence compared to the long limb i.e. the observed minor folds are parasitic to larger slump structures. However, the folds in this study are not positioned on short limbs, and in addition clearly rework and therefore post-date the typically larger and structurally underlying downslope (NE-verging) folds.

5.2. A reversal in the component of shortening

A new component of shortening may be caused by an anti-dislocation compressive wave (Farrell, 1984) migrating back up the slump during cessation of movement at the toe (see Alsop and Marco, 2011). However, migration of an anti-dislocation wave will not necessarily create a reversal in vergence. In addition, only the upper parts of the individual slumps are affected by reversals in vergence rather than the entire slump as would be expected with an anti-dislocation system.

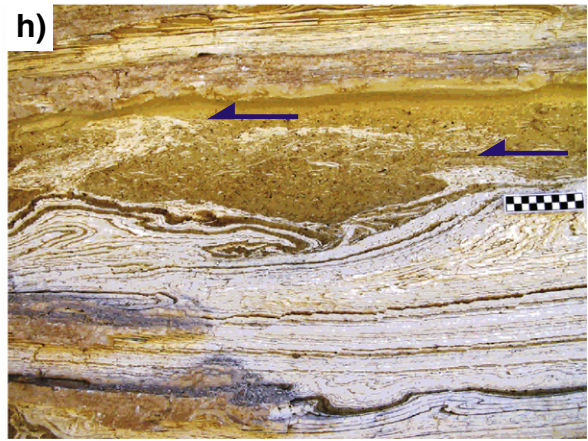
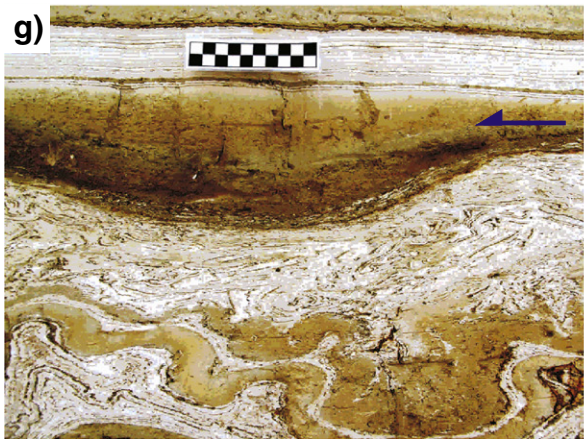
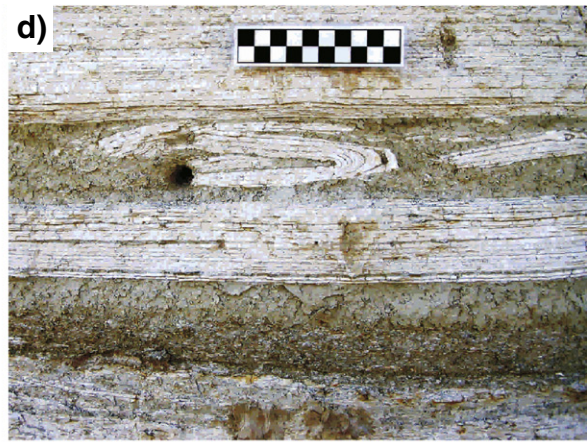
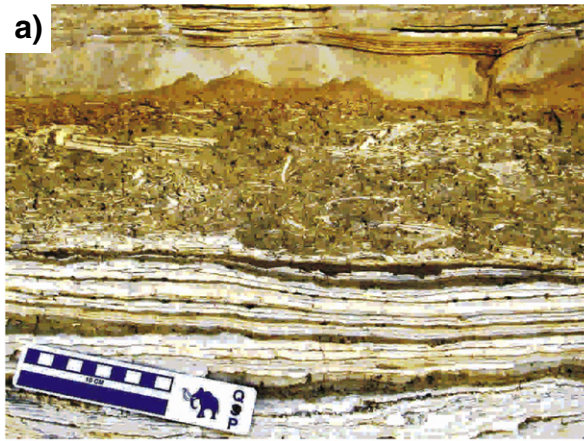
5.3. A reversal in the local slump direction

Partial reversals in the slump direction may be caused by gravity-driven flow of sediment off structural culminations or “highs” created during the initial downslope slump event. This secondary slumping would be marginally later than the initial event, and only locally produce upslope vergence where sediment is itself dipping upslope off crests. In addition, upslope verging fold hinges statistically display the same orientation as the downslope verging folds, as would be expected during secondary slumping off structural highs created by broadly cylindrical primary slump folds. These relationships, together with the observation that sediments, and in particular mud-rich units, may dramatically thicken towards the synclinal troughs suggests that such secondary slumping may be one of the mechanisms for minor folds and thrusts to verge back upslope. However, the intensity of such structures is typically limited, and they are only very locally developed during relaxation of earlier culminations (see Alsop and Marco, 2011).

5.4. A reversal in relative motion within the slump

Reversals in relative motion (and hence vergence) may be caused by the underlying parts of a slump moving downslope more rapidly than the overlying parts (see also Strachan & Alsop, 2006). The main slump and the folds displaying opposing vergence would therefore be of the same age. Dasgupta (2008) notes that if a layered stack of sand and clay flow down a slope, the viscosity contrast between the units generates different velocities leading to deformation and folding of the rheological interface. The application of simple shear (e.g. Woodcock, 1976b) results in amplification and overturning of these folds. The deeper parts of a slump would therefore need to move more rapidly to create folds locally verging upslope. This may also happen if thrusts within a slump are “pinned” (Strachan and Alsop, 2006). However in the present case, the NE-verging slump folds are locally reworked by upslope verging structures indicating a distinct temporal sequence, rather than synchronicity as implied in this model.

Fig. 7. a) Breccia unit containing aragonite fragments and capped by a clastic horizon. b) Irregularly truncated aragonite layers overlain by a dark clastic horizon containing aragonite fragments. c) Breccia layer displaying increasing disaggregation upwards into a dark clastic unit (below scale). The dark clastic layer above the scale shows variably orientated aragonite fragments. d) Folded aragonite fragments incorporated into a breccia layer (below scale). e) Deformed layers interfolded with overlying breccia, indicating that folding continued after brecciation. Breccia and deformed layers are then truncated by the overlying clastic horizon that contains two distinct laminae of aragonite fragments indicating multiple pulses of flow. f) Upright fold flanked by recumbent folds closing in opposite directions suggestive of instability and dewatering. These structures are truncated by the overlying clastic horizon (with scale). g) Dark clastic layer (below scale) displays extreme thickness variation to infill topography. The clastic unit is graded, with coarse aragonite fragments concentrated on the steeper SW-facing slopes, suggesting SW-directed flow during deposition of the unit. h) NE-verging folds capped by a graded clastic unit that infills local topography. Note that SW-verging folds are picked out by lighter aragonite-rich layers in the clastic layer. In each case, the scale is shown by a 10 cm long chequered ruler or 15 mm diameter coin.



5.5. A reversal in relative velocity against an ambient fluid

Martinsen (1994) summarises mass movement deformation of sediments and notes that slumps represent coherent masses with considerable internal deformation, and form part of a continuum from (slow) creep and slides through to flows marked by plastic or fluidal behaviour associated with (rapid) turbulent flow. It has been shown experimentally (e.g. Postma et al., 1988) that sediment-laden turbulent flow is capable of generating reversals in shear along its upper margin where its velocity is reduced via contact with the overlying ambient fluid (see Mulder, 2011 p.34). As the NE-directed slump at Peratzim contains coherent bedding that defines intricate structural detail, and does not comprise sediments that have been deposited from suspension, it cannot be described as a fluidal flow that is turbulent and carries material in suspension. As such, the velocity of slumping is considered too low and would be incapable of developing notable reversals in shear at the upper contact where it comes into contact with the ambient fluid. Existing downslope verging folds are clearly reworked by the upslope verging folds resulting in fold interference patterns (see Section 4.5). This demonstrates that such folds reflect a direct temporal relationship and are not created by shearing against an ambient fluid. In addition, multiple reversals in vergence and shear are also observed suggesting a more complex history than shearing against an ambient fluid.

Thus, the observation that the underlying slumps typically form coherent and ordered fold and thrust geometries, suggests that the velocity of slumping was relatively low. In addition the correspondence of slumped stratigraphy with that of underlying beds suggests that the slumps are not far-travelled. The fact that the downslope directed slumps are not turbidites effectively dismisses the notion that upslope verging folds are generated by shear against the ambient fluid during (rapid) downslope movement.

5.6. A reversal in the direction of flow caused by a reflected turbidity current

Gravity-driven slumped sediments may evolve or transform into sediment-laden turbulent flows that continue to move rapidly downslope due to suspended sediment increasing the density of the flow compared to the surrounding water (e.g. see Strachan, 2008 and references therein). A reversal in flow direction or “back wash” is created by a turbid flow reaching the opposing margin of a confined basin, and then being reflected back over to the original site (e.g. Allen, 1982 p. 236). This effect may occur when the basin is much narrower than the potential travel distance of the flow, or if a significant bathymetric obstacle exists in the path of the flow. However, as Lake Lisan is considered to be a deep basin with maximum water depths of between 300 m and 450 m (Ichinose and Begin, 2004, page 9) and dense hyper-saline brines at depth, the likelihood of a turbid flow having the energy to travel back up the pronounced margins of the trough may be considered more limited. In addition, increasing shear culminating in brecciation of layers directly overlying the upslope verging folds is difficult to reconcile with a “reflected flow” model. A reflected turbidity current may maintain energy (e.g. Kneller, 1995), but could not gather more energy than the initial slump event itself (as suggested by the brecciation of layers above the slump but not within it). There is no evidence of slumps or turbid flows carving channels in the Lisan Formation that may concentrate or focus return flows into the Peratzim area and increase their energy. Reflected flow may

be in any orientation relative to the original turbid flow depending on the geometry and orientation of the reflecting obstacle. There is therefore no necessity for reflected flow to display similar trends (with a reverse polarity in flow direction). The hypothesis that the opposing margin of the basin may reflect NE-directed turbid flow (associated with slumping) directly back upslope towards the SW is therefore considered unlikely.

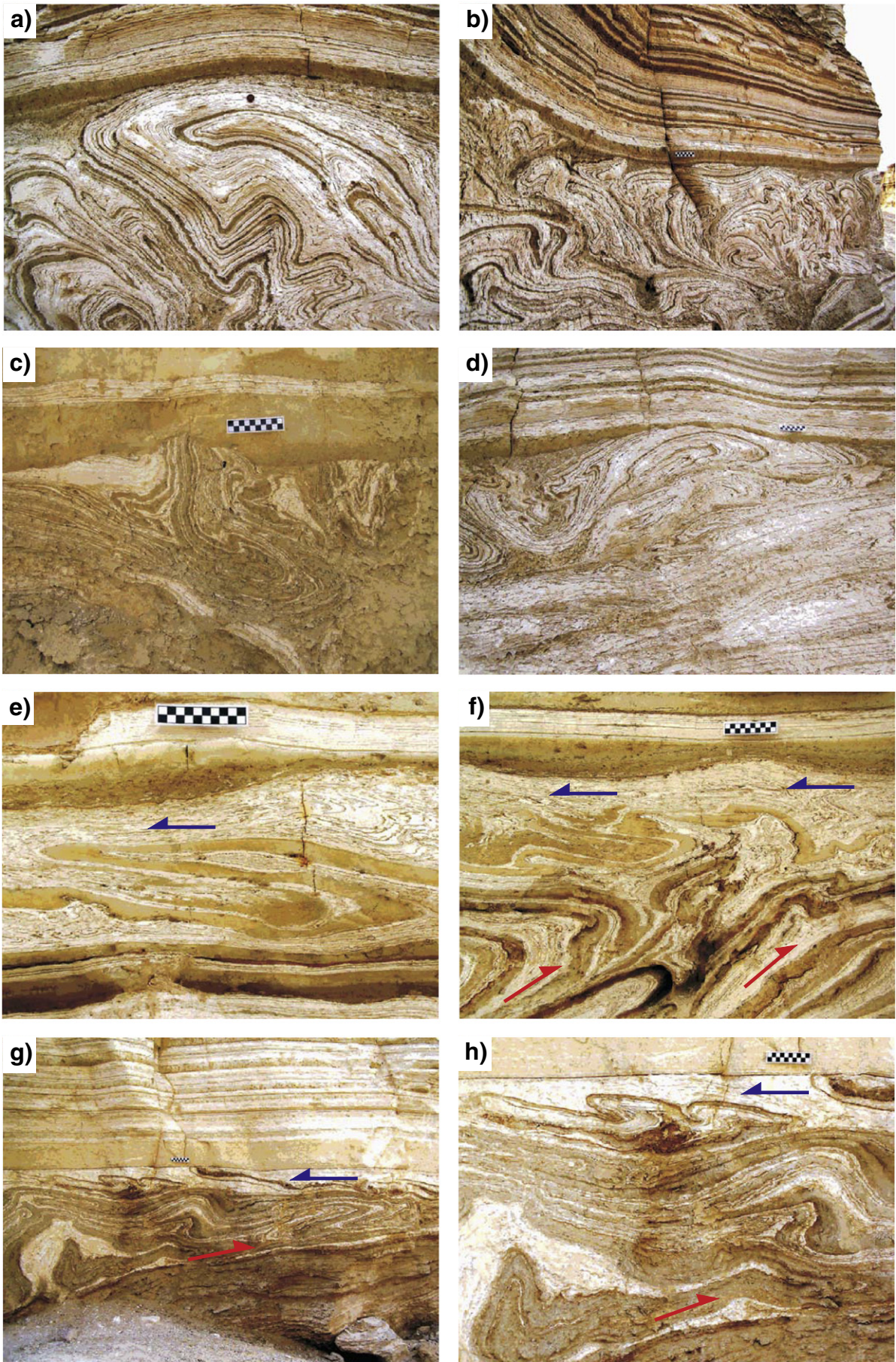
5.7. A reversal in the direction of flow caused by a tsunami or seiche

The reversal in minor fold and thrust vergence directly above the NE-directed slump structures at Peratzim may represent the effects of fault motion directly on the floor of the lake and/or an earthquake triggering a sub-aqueous landslide that generates a tsunami event. Tsunamis within enclosed lakes are typically referred to as the initial wave produced by displacement normally triggered by an earthquake, and a seiche is the harmonic resonance of waves within the lake as the water then “sloshes” back and forth (e.g. Ichinose et al., 2000). A tsunami is typically generated by displacement of the sea/lake floor, and may create a current that flows directly upslope thereby shearing underlying sediments in the opposite direction to the “normal” gravity-driven downslope slumping (Figs. 7, 8). Both tsunami and seiche waves would, due to the travel time, arrive slightly later than the main slump event and therefore rework the top of the entire slumped unit. This model is broadly consistent with our observations and we shall now discuss it, together with further evidence for seiche and tsunami in the Dead Sea Basin, in greater detail.

6. A model of fold and fabric relationships through the deformed horizon

We here suggest that the detailed observations listed in Section 4 above are consistent with a seismically triggered tsunami event whereby the initial earthquake almost instantaneously generates downslope slumping of sediment marked by NE-verging fold and thrust packages (Fig. 11). The same seismic trigger may generate a tsunami via direct fault displacement of the lake floor and/or sub-aqueous landslide within the basin (Fig. 12a). Significant normal faulting during deposition of the Lisan Formation has been reported by Marco and Agnon (1995) and may include structures such as the Jericho Fault that currently lies in the centre of the Dead Sea, and which is also thought to broadly coincide with the centre of the ~20 km wide Lake Lisan. The displaced water column will arrive fractionally later at the slumped mass due to its travel time of just a few minutes. The tsunami wave will move directly up the shallow slope (due to refraction) and increase in amplitude as the depth of water decreases (Fig. 12b). A tsunami moving through 50 m of water will affect the entire water column and travel at ~80 km/h which will impart a significant shear stress on the underlying unconsolidated slumped sediments. This flow of water back up the shallow slope of the slumped Lisan sediments may thereby generate minor folds and thrusts within the top 30 cm of sediment, with shear stress increasing upwards towards the water-sediment interface (Fig. 11). Such an upward gradient in shear stress is difficult to explain by secondary slumping, as the shear stress would in this case increase downwards towards an underlying detachment. Current reworking of the top ~30 cm of sediment is also observed in other settings where cross beds may be deformed and reworked by shear stresses initiated by water flow (e.g. Nichols, 2009 p. 277). Any evacuation and withdrawal of water

Fig. 8. a, b) Isoclinal folds overlain by a breccia and capped by a dark clastic horizon. c) Deformed unit displaying abrupt truncation of layering by the overlying clastic horizon (with scale). This graded clastic unit infills the slump-related topography. d) Recumbent isoclinal fold (below scale) displaying truncation of the upper fold limb that is then capped by a dark clastic horizon. e) SW-verging isoclinal fold (developed above NE-verging folds shown on Fig. 3b) which grades upwards into a breccia and is capped by a dark clastic unit (below scale). The clastic unit is graded, displays variable thickness to infill underlying topography, and has coarser aragonite fragments concentrated on the steeper SW-facing slopes, suggesting SW-directed flow during deposition of the unit. f) SW-verging folds overlain by a breccia and capped by a graded clastic horizon (below scale) that infills underlying topography. g) NE-verging folds and thrusts overlain by SW-verging folds (below scale). The deformed horizon is then capped by a thick (~25 cm) clastic horizon. Detail of this folding is shown in h). In each case, the scale is shown by a 10 cm long chequered ruler or 15 mm diameter coin.



prior to the tsunami surge may also create downslope verging structures that may be difficult to separate from the primary slump structures. In addition, the deformed horizon at Peratzim may have been in too great a depth of water to be affected by such an evacuation.

As the tsunami moves directly up the dip of the shallow slope, the folds it produces are broadly coaxial to those created by sediment slumping directly down the same slope. In this case, the refolding of the upper parts of upslope verging folds, together with the more common chaotic sediments and breccia that directly overlie them may be created by the flow of water as the tsunami surge eventually drains and rushes back to the lake (Figs. 11, 12c). The reworked upper parts of the slump are overlain by a distinct undeformed capping unit comprising graded silt containing aragonite fragments (Fig. 11). In some cases the underlying slump structures are truncated by the capping unit, whilst in others there is a transition into the breccias and cap (Figs. 11, 12d). We propose that these different relationships are simply a consequence of the intensity of the tsunami or seiche current, with an erosive truncation suggesting that the tsunami backwash or seiche wave may have been locally more intense. The concentration of coarser aragonite fragments on the SW side of obstructions, together with SW-verging recumbent folds suggests SW (upslope) -directed flow during initial deposition of the capping unit. This is difficult to reconcile with a turbidity current scenario that would be associated with downslope flow.

The mechanics of shear instability at the water–sediment interface have been modelled using the Kelvin–Helmholtz instability formulation by Wetzler et al. (2010). According to their model we observe a stage in which the shear had evolved to complete instability at the interface and the resultant turbulence is manifest in the form of breccia, i.e., the upper parts of the horizon appear fragmented and even pulverised, with fine silts and muds that were deposited from suspension during a period of quiescence following the tsunami and seiche waves. Further observations and evidence concerning the operation of tsunami and seiche waves in the Dead Sea Basin are now presented.

6.1. Records of tsunami and seiche in the Dead Sea

Historical reports associate large waves in the Dead Sea, possibly seiches, with earthquakes that were felt and inflicted damage in the region. Catalogues of ancient earthquakes list the CE 363, 749, 1546, 1837, and 1927 events (Amiran et al., 1994; Ambraseys, 2009). The 363 wave is reported from the southern part of the Dead Sea (Shalem, 1956), whilst the earthquake rupture of 749 was found in the Jordan Valley and reported to have been accompanied by a large wave (Ben-Menahem, 1991). The 1546 earthquake is also reported to have triggered a large wave (Shalem, 1956), although later studies conclude that it was a rather small-sized earthquake (Ambraseys and Karcz, 1992). The earthquake of 1837 was in southern Lebanon (Ambraseys, 1997; Nemer and Meghraoui, 2006) but coastal subsidence and waves were reported from the Dead Sea (Amiran et al., 1994). The 1927 earthquake also triggered a small wave in the northern Dead Sea that was directly witnessed (Shapira et al., 1993). There is thus abundant historical and directly-witnessed evidence of large seiche and tsunami waves in the Dead Sea.

6.2. Breccia and gypsum records of tsunami and seiche waves in the Dead Sea

The generation of seismite breccia layers by tsunami or seiche waves has been proposed previously in the Lisan Formation by Marco and Agnon (1995) and Agnon et al. (2006). About a third of these breccia layers are capped by gypsum, with precipitation of gypsum requiring the mixing of otherwise stratified water in the lake (Ichinose and Begin, 2004; Begin et al., 2005). This overturn and mixing of the water column is considered to be the result of seiches

generated by earthquake ruptures along the lake bottom, with the breccia-gypsum association resulting from stronger and/or closer earthquakes. The breccia units recorded by Begin et al. (2005) are typically overlain by detritus interpreted as being deposited by tsunami or seiche waves. Begin et al. (2005) also model earthquakes from the thickness of these breccia horizons and suggest magnitudes of 7.1–7.4 with a background recurrence interval of 11 ky since 40 ka. No gypsum association has been observed above the breccia layer in the Peratzim case study.

6.3. Numerical models of tsunami and seiche waves in the Dead Sea

Although it is beyond the scope of this paper to discuss detailed numerical modelling of seiche and tsunami waves, it is important to note that Ichinose and Begin (2004) undertook numerical simulations of tsunami generation in Lake Lisan and the Dead Sea. They suggest that a credible magnitude 7.3 earthquake in the centre (depocentre) of Lake Lisan could have generated an 8–10 m high tsunami wave (and >4 m on average) along its shoreline. The associated seiche in Lake Lisan is calculated by Ichinose and Begin (2004) to last >2 h.

7. Discussion

7.1. Could deformed horizons be created by storm waves in the Dead Sea?

The depth of water is critical in determining the influence and effects of storm waves on sediments, with overall criteria for distinguishing between storm and tsunami deposits being reviewed in detail by Morton et al. (2007). Agnon et al. (2006) suggest that water depth in Lake Lisan was “several tens of metres” and the effects of storm waves on the Lisan Formation may therefore have been limited. Importantly, the lack of sedimentary structures such as cross laminations indicates that the Lisan Formation at Peratzim was deposited below wave base in water too deep (>30 m) to be influenced directly by storms. As noted above in Section 3, the Lisan Formation at Peratzim is therefore considered to have been deposited in water depths of between 30 and 100 m. It should also be noted that the effects of storm waves will also be diminished in the enclosed Lake Lisan due to their limited fetch and shorter wavelength (that dramatically reduces the period of increased water pressure—see Section 7.3 below).

Gardosh et al. (1990) state that Lake Lisan covered the marginal Dead Sea fault system, and Marco and Agnon (1995) discovered syn-depositional faulting at the bottom of the lake about 1 km east of the marginal fault near Masada, which displaced the lake floor. The capability of these seismically active faults to generate tsunami and seiche waves may be further enhanced by the enclosed nature of the basin. It should be noted that a tsunami wave affects the entire water column (e.g. Morton et al., 2007) and therefore its effects on sea floor sediment are not so water depth-dependent as standard storm waves. In summary, the lack of sedimentary structures such as cross bedding indicates that the depth of water in which the Lisan Formation at Peratzim was deposited was too great to be affected by storm waves. It is however entirely possible that seiche and tsunami waves could directly affect the Lisan Formation and this is now discussed in greater detail.

7.2. Are tsunami and seiche waves capable of deforming deeper water sediments?

The effectiveness of seiche and tsunami waves in deforming sediments will depend on a number of variables including current velocity, water depth, and the strength and cohesiveness of the sediments. Current velocity immediately above the sea bed may be slightly retarded due to friction and is dominated by laminar flow in deeper

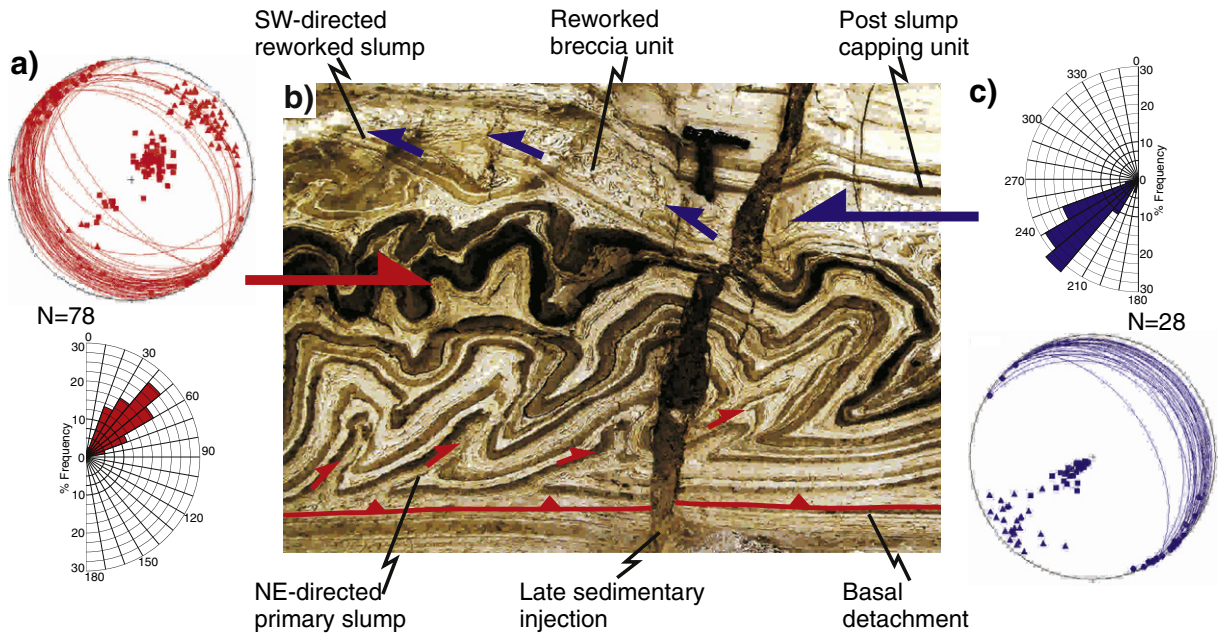


Fig. 9. Summary stereonets, rose diagrams and photograph showing NE-verging slumps overlain by SW-verging structures and breccia. Both sets of structures are cut by a sedimentary injection. Scale is shown by the 30 cm long hammer. Stereonets and rose diagrams of NE-directed slump fold data (a) and overlying SW-verging folds (c) are shown on photograph b). Facing directions are also highlighted on the associated rose diagrams, with NE-facing folds on a) (in red) and SW-facing on c) (in blue). Equal area stereoplots show fold hinges (circles) and axial surfaces displayed as both great circles and squares representing poles. Upward facing directions are plotted as solid triangles which are projected vertically down (as chordal points) from their upper hemisphere intersection onto the lower hemisphere stereonet.

water and by more turbulent flow in shallower water (<200 m) where significant shear stress may develop along the sediment surface (Sugawara et al., 2008). In Japanese examples of tsunami transport of foraminifera that are developed on the seabed at depths of 45–90 m indicates current velocities of 0.2–0.5 m/s at these depths after a magnitude 7.8 earthquake (Nanayama and Shigeno, 2006). Although macro-faunal content of tsunami deposits has been used as a diagnostic feature to indicate where deeper water sediments (and fauna) have been transported to shallower settings, they are clearly of no value in the lifeless Dead Sea which contains no such fauna. However, magnitude 7.3 earthquakes are considered credible and have been numerically modelled for the Dead Sea (Ichinose and Begin, 2004), whilst the suggested water depths of between 30 and 100 m during deposition of the Lisan Formation at Peratzim are

similar to water depths marked by scouring and deformation of the sea bed in the Japanese example (Nanayama and Shigeno, 2006).

The strength and cohesion of sediment is highly variable with fine sand requiring the minimum current velocity for transport, whilst clay and silt have a much higher resistance to currents with mud on the deeper sea floor difficult to move even by a tsunami (Sugawara et al., 2008 and references therein). However, calcareous muddy sediment (perhaps not dissimilar to marls of the Lisan Formation) is eroded by a current exceeding 0.15 m/s as reported by Kastens and Cita (1981). Whilst increased cohesion may also develop via biological agents (e.g. Noda et al., 2007), this may be limited in hypersaline waters such as those in Lake Lisan. These general observations on current velocities, water depths and cohesiveness of sediments collectively suggest that it is entirely possible for the Lisan Formation at

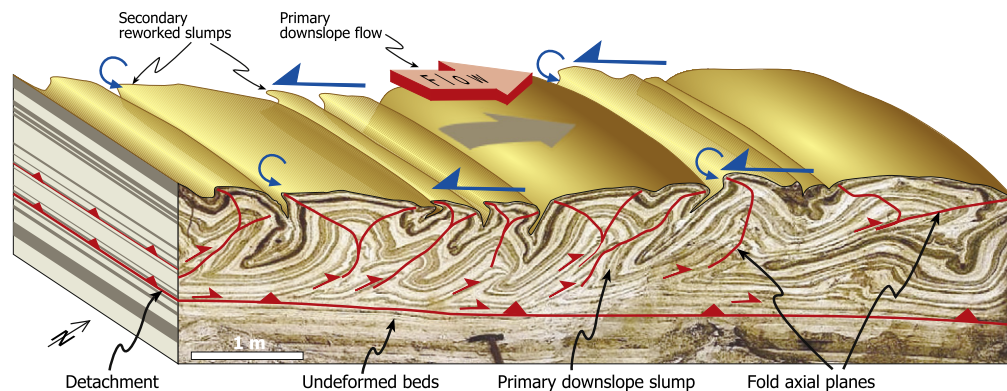


Fig. 10. Photograph and schematic interpretative top surface of a metre-scale fold and thrust system translating downslope towards the NE. The ~13 m section comprises upright folds that develop above an undeformed sequence. The box folds typically display bifurcating axial planes (highlighted in red) that root downwards onto an underlying detachment. Vergence towards the NE associated with primary downslope flow becomes more pronounced towards the left-hand side of the image where thrusting is observed. The upper parts of these primary structures are reworked by secondary shear (highlighted by blue arrows) associated with upslope flow directed towards the SW.

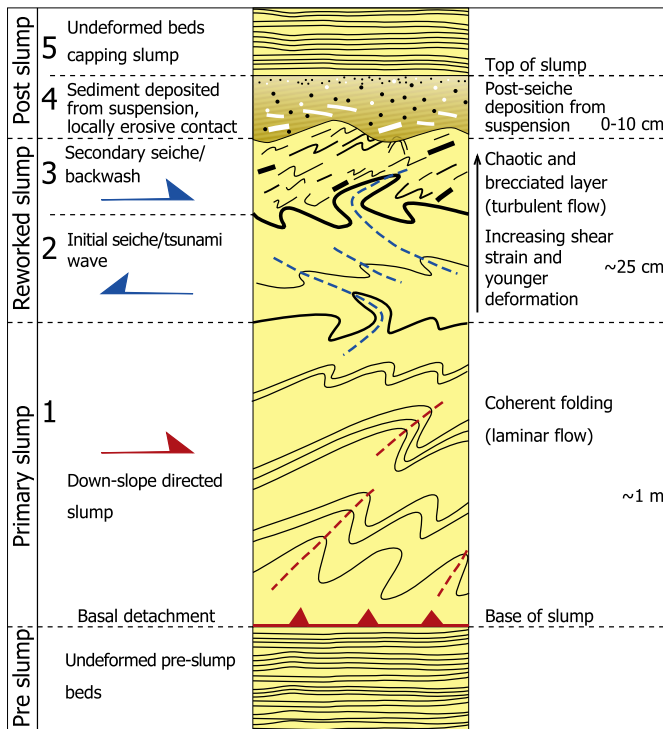


Fig. 11. Schematic sedimentary and structural log summarising features associated with slumping. Pre-slump beds beneath the basal detachment remain undeformed, whilst beds within the overlying primary slump deposits display downslope verging folds and thrusts (1). The upper parts may form a reworked slump deposit with an initial incoming seiche/tsunami wave creating upslope verging structures (2), that are succeeded and reworked by a secondary backwash associated with outgoing flow that may become locally erosive (3). Sediment that has been carried in suspension is deposited during post slump quiescence to create graded beds that infill local topography and mark the top of the slump and seiche event (4). Normal deposition resumes resulting in undeformed beds that overlie the slump (5).

Peratzim to have been deformed and eroded by tsunami and seiche waves.

7.3. How do tsunami and seiche waves facilitate deformation of sediments?

It has long been recognised that one of the principal mechanisms to reduce the shear strength of sediments and thereby facilitate their deformation is to increase pore fluid pressure (e.g. Maltman, 1994b and references therein). It is therefore notable that pressure pulses associated with small 1–2 m tsunami waves on the sea bed are approximately double those of swell and storm waves of similar size (Bryant, 2001 p. 38). The relative pressure pulse of tsunami waves compared to storm waves actually increases with water depth, with a 1 m tsunami wave creating a greater pressure pulse than 4 m storm waves at water depths of 100 m as envisaged for the Lisan Formation at Peratzim (Bryant, 2001 p.39). In addition, it has been calculated that a 5 m high tsunami wave will generate a pressure pulse capable of causing compacted muds to fail on the sea bed at water depths of 100 m (Bryant, 2001 p. 39). However, one of the most significant factors is that pressure increases associated with shearing of the sea-bed by tsunami may last for several minutes (Bryant, 2001 p.40) enough to facilitate liquefaction (e.g. Fig. 7f). The shear between the water body and the lakebed would create folds that evolve, increase in size, with their upper parts ultimately becoming unstable (Heifetz et al. 2005; Wetzler et al. 2010). Thus, it has been theoretically shown that tsunami waves in deeper water (~100 m) settings not only effectively increase fluid pressure to encourage further weakening of sediment over a period of time, but

also simultaneously increase shear stress along the sediment water interface that we suggest would facilitate folding.

7.4. Does seismicity or slumping trigger tsunami and seiche waves?

Submarine slides and slumps may displace significant volumes of material and thereby induce tsunami in their own right, which are typically smaller than those created by seismic displacement of the sea-bed (Bardet et al., 2003). Within the Lisan Formation, it is unlikely that the downslope slump itself caused a tsunami because a) the palaeoslope was very gentle with dips of $<1^\circ$ to drive slumping,

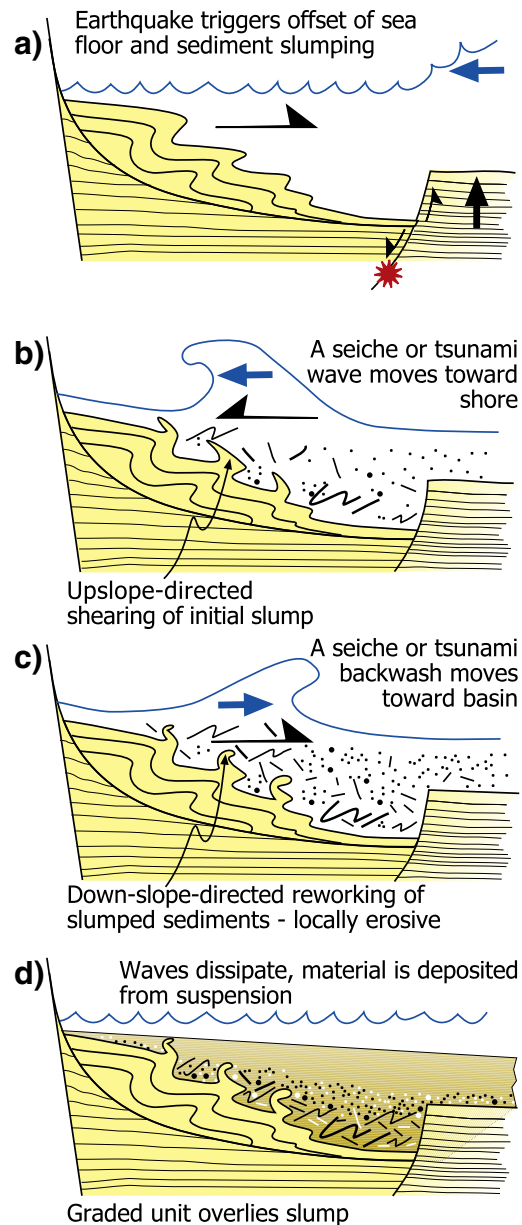


Fig. 12. Schematic cartoons summarising the sequential evolution of slump and tsunami/seiche related deposits. a) Fault movement (marked by an earthquake) causes offset of the sea floor that displaces the overlying water column thereby generating a tsunami and seiche waves. The same earthquake triggers downslope slumping of sediments in adjacent areas. b) The tsunami and seiche wave arrive immediately after slumping and move towards the shore, resulting in upslope directed shearing and reworking of initial slump folds. c) The outgoing seiche or tsunami backwash causes downslope directed shearing of reworked sediments, which may locally become erosive. d) As the seiche waves dissipate, sediment is deposited from suspension resulting in a graded bed that caps the underlying deformed and locally scoured slumped unit and also infills local topography.

b) the slump is structurally well-ordered and coherent and would not move rapidly enough, and c) the observed slumps are relatively small and do not appear to contain a large enough volume of material. Faulting has clearly affected the sea floor and deposition of the Lisan Formation at Masada to generate seismites (e.g. Marco and Agnon, 1995; Alsop and Marco, 2011 p.444). In addition, bitumen which is directly observed along fault planes has also been observed to rise up into the Dead Sea after earthquakes, suggesting that faults may have ruptured the sea floor and directly released buoyant bitumen into the water (e.g. Nissenbaum, 1978; Beinn and Amit, 1980). Therefore a model in which a single seismic event not only ruptured the sea floor to create a tsunami, but also directly triggered downslope slumping in the Lisan Formation is preferred.

This model described above and in Section 6 is different to that envisaged by Sarkar et al. (2011) for slump related folding generated by an ancient tsunami in India. They suggest that downslope directed folding was developed within tsunami-deposited muds formed in a beach environment by the action of an intense backwash. Clearly the depositional environment they describe is very different to the offshore setting of Peratzim, with folding and deformation at Peratzim being truncated by, and therefore predating deposition of capping muds. Sarkar et al. (2011) do not report any on shore directed folding, perhaps suggesting that in this case the backwash was more intense than the original tsunami and/or that the newly deposited and relatively weak muds were required to record folding.

7.5. Do capping sediments above reworked slumps represent homogenites?

The effects of tsunami in deeper water settings are typically considered to be marked by a blanketing layer of graded sand and mud termed a homogenite that may be linked to an individual tsunami event (e.g. Cita et al., 1996). Studies of the recent 2010 Haiti earthquake indicate that a large sediment plume was still depositing mud long after the cessation of tsunami and seiche waves and up to 2 months after the seismic event itself (McHugh et al., 2011). Multiple tsunami or seiche waves will typically therefore not have chance to deposit multiple layers of sand or silt and clay as the settling velocities are slower than the recurrence interval of the seiche wave (e.g. Bourgeois et al., 1988). Deposits associated with seiche and tsunami are therefore typically capped by a single clastic homogenite (Cita et al., 1996). It is therefore notable that the reworked slump at Peratzim is capped by a single graded clastic unit up to 30 cm thick, that could be interpreted as a homogenite. Mud rip-up clasts observed within homogenites are represented within the Peratzim example by aragonite fragments up to 5 cm in length, that define an overall single graded unit. The observation that NE-verging slumps and the overlying SW-verging folds are not separated from one another by a breccia or homogenite horizon supports the interpretation that they are created by the same earthquake and do not in this case represent multiple seismic events concealed within the same horizon (see Alsop and Marco, 2011). The lack of breccia between NE-directed slumps and overlying SW verging folds also demonstrates that the actual slumps were relatively slow moving and incapable of generating turbulent flow associated with shear against an ambient fluid. This may indicate that in this case, the capping layer was not created by a turbid flow developed from the underlying slump (see Strachan, 2008).

The marked coincidence of thick capping units directly overlying slumps also suggests that they do not in this case relate to seasonal variations, where clastic material is washed into the basin and deposited during winter storms (Begin et al., 1974). We consider that seismogenic breccia layers are deposited from suspension from tsunami and seiche currents, as they markedly thicken on the downthrown side of faults that cut the sea floor to create growth strata (Marco and Agnon, 2005) (Fig. 12). Local slumping down the fault scarp may also subsequently affect the breccia layers and highlights local sea floor topography created by faulting. In summary we suggest

that the capping homogenite is directly associated with the slumping process itself, and represents material that has been eroded from the upper surface of the slump by the action of seiche and tsunami waves and then deposited from suspension as wave action dissipates.

7.6. Why is there only limited terrestrial input from seiche and tsunami backwash?

Tsunami backwash flows in beach and near shore settings may contain coarse clastic detritus (e.g. Fujiwara and Kamataki, 2008) and may be stronger than the original tsunami where they are channelized into certain locations. Such flows may rework sediment deposited by the initial tsunami surge, and also wash wood and terrestrial vegetation back into the basin. Within the Dead Sea shore and near shore environment however, there is a distinct lack of vegetation and wood available for such reworking because of the extreme aridity, coupled with the saline conditions. However, fragments of wood deposited in Holocene seimite layers were interpreted as drift wood and have been used for C¹⁴ dating (Kagan et al., 2011). We suggest that such fragments of wood were actually washed into the seimite deposit by the backwash action of tsunami and seiche waves on the terrestrial near shore environment.

It is apparent that the capping homogenite at Peratzim contains little coarse clastic beach detritus. We suggest this may reflect a number of factors including:

- The case study area at Peratzim is considered to lie in water depths of 30–100 m when slumping and tsunami/seiche waves occurred. As such, it is further removed (>2 km) from coastal and near shore environments than typically reported tsunami and seiche deposits.
- The shoreline of Lake Lisan was partially cemented by aragonite crusts forming a “hard beach rock” up to a few tens of cm thick (Bookman et al., 2004). This means that cemented sands and gravels (as developed along the shore today) will not easily wash back as observed in typical tsunami deposits (e.g. Scheffers and Kelletat, 2003).
- If sea levels were falling then a steep stepped beach profile is produced (as observed today) that would significantly limit the advance of a tsunami or seiche wave. The aragonite cementation noted above may also encourage steeper profiles to be stable and preserved.
- The laminated aragonite rich layers are both competent and coherent so that they may fracture and break into fragments to form breccias, whilst the finer clastic muds are dispersed. Aragonite clasts within the capping homogenite may therefore represent the products of backwash. We therefore suggest that distinct horizons of coarse clastic detritus and pebbles from the beach environment may not be diagnostic of tsunami and seiche backwash in this particular case study from the Dead Sea Basin.

8. Conclusions

The slumped horizons at Peratzim may be divided into 3 main units comprising a) a lower primary slumped unit dominated by downslope (NE) verging structures, b) an overlying reworked unit with structural vergence both up (towards the SW) and down the palaeoslope associated with a higher energy event and sometimes culminating in a distinct breccia horizon, c) a largely undeformed post-slump capping horizon that may locally truncate underlying structures and is considered to represent a homogenite. The pattern of refolding and reworking clearly indicates that the SW-directed (upslope) shearing post-dates the original NE-verging slump event, but displays no intervening breccia and is therefore in direct structural continuity. SW verging structures are themselves locally reworked by subsequent NE-directed folds, suggesting a systematic reversal in

vergence associated with switching in flow directions up through the reworked slump and breccia unit. Perhaps one of the most likely scenarios to generate such relationships in the present case study are seismically triggered tsunami and seiche waves that are considered to immediately post-date the slump event triggered by the same earthquake.

The seiche and tsunami hypothesis is also supported by a number of additional observations and interpretations including: a) It is already well established that seismogenic seiche waves operated within Lake Lisan and may generate intraformational breccia layers within the Lisan Formation (e.g. Marco and Agnon, 1995). b) Faults are marked by local thickening and growth strata within the Lisan Formation indicating that they directly displaced the lake floor (which also occasionally released bitumen up into the water column). c) The capping of seismogenic breccia layers by gypsum horizons has previously been interpreted as a product of mixing of the entire water column by associated tsunami and seiche waves (Marco and Agnon, 1995). d) Detailed numerical modelling already suggests that a credible magnitude 7 earthquake would create an 8–10 m high tsunami wave and a seiche lasting more than 2 h in the Dead Sea Basin (e.g. Ichinose and Begin, 2004). e) Tsunami waves have been directly observed in the Dead Sea following a number of historical earthquakes (Niemi and Ben-Avraham, 1994).

Thus, although tsunamis have previously been both numerically modelled and directly observed in the Dead Sea Basin, this study forms the first detailed observation and structural interpretation of potential reworking associated with such seismogenic tsunami and seiche waves in offshore settings. Importantly, the preservation potential in the geological record of such offshore deposits is much greater than that of tsunami events observed in the coastal environment.

Acknowledgments

We thank Mr. John Levy, together with the Carnegie Trust and the Royal Society of Edinburgh for travel grants to IA, and the Israel Science Foundation for grant 1539/08 to SM. SM also thanks the Department of Earth Sciences at Durham University for hosting a visit and facilitating this paper. We thank Tim Debacker and an anonymous reviewer for comments on versions of this paper.

References

- Agnon, A., Migowski, C., Marco, S., 2006. Intraclast breccia layers in laminated sequences: recorders of paleo-earthquakes. In: Enzel, Y., Agnon, A., Stein, M. (Eds.), *New Frontiers in Dead Sea Paleoenvironmental Research: Geological Society of America Special Publication*, pp. 195–214.
- Allen, J.R.L., 1982. Sedimentary structures, their character and physical basis. *Developments in Sedimentology*, 30. Elsevier, Amsterdam, 663 pp.
- Alsop, G.I., Carreras, J., 2007. Structural evolution of sheath folds: a case study from Cap de Creus. *Journal of Structural Geology* 29, 1915–1930.
- Alsop, G.I., Holdsworth, R.E., 2002. The geometry and kinematics of flow perturbation folds. *Tectonophysics* 350, 99–125.
- Alsop, G.I., Holdsworth, R.E., 2004a. The geometry and topology of natural sheath folds: a new tool for structural analysis. *Journal of Structural Geology* 26, 1561–1589.
- Alsop, G.I., Holdsworth, R.E., 2004b. Shear zone folds: records of flow perturbation or structural inheritance? In: Alsop, G.I., Holdsworth, R.E., McCaffrey, K.J.W., Hand, M. (Eds.), *Flow Processes in Faults and Shear Zones: Geological Society of London Special Publication*, 224, pp. 177–199.
- Alsop, G.I., Holdsworth, R.E., 2007. Flow perturbation folding in shear zones. In: Ries, A.C., Butler, R.W.H., Graham, R.D. (Eds.), *Deformation of the Continental Crust: The Legacy of Mike Coward: Geological Society, London, Special Publications*, 272, pp. 77–103.
- Alsop, G.I., Marco, S., 2011. Soft-sediment deformation within seismogenic slumps of the Dead Sea Basin. *Journal of Structural Geology* 33, 433–457.
- Alsop, G.I., Marco, S., 2012. A large-scale radial pattern of seismogenic slumping towards the Dead Sea Basin. *Journal of the Geological Society of London* 169, 99–110.
- Alsop, G.I., Holdsworth, R.E., McCaffrey, K.J.W., 2007. Scale invariant sheath folds in salt, sediments and shear zones. *Journal of Structural Geology* 29, 1585–1604.
- Ambraseys, N., 1997. The earthquake of 1 January 1837 in southern Lebanon and northern Israel. *Annali di Geofisica* 40, 923–935.
- Ambraseys, N.N., 2009. *Earthquakes in the Mediterranean and Middle East: A Multidisciplinary Study of Seismicity up to 1900*. Cambridge University Press, Cambridge, 947 pp.
- Ambraseys, N., Karcz, I., 1992. The earthquake of 1546 in the Holy Land. *Terra Nova* 4, 253–262.
- Amiran, D.H.K., Arie, E., Turcotte, T., 1994. Earthquakes in Israel and adjacent areas: macroseismic observations since 100 B.C.E. *Israel Exploration Journal* 44, 260–305.
- Bardet, J.-P., Synolakis, C.E., Davies, H.L., Imamura, F., Okal, E.A., 2003. Landslide tsunamis: recent findings and research directions. *Pure and Applied Geophysics* 160, 1793–1809.
- Bartov, Y., Steinitz, G., Eyal, M., Eyal, Y., 1980. Sinistral movement along the Gulf of Aqaba—its age and relation to the opening of the Red Sea. *Nature* 285, 220–221.
- Bartov, Y., Goldstein, S.L., Stein, M., Enzel, Y., 2003. Catastrophic arid episodes in the Eastern Mediterranean linked with the North Atlantic Heinrich events. *Geology* 31, 439–442.
- Beck, C., 2009. Late Quaternary lacustrine paleo-seismic archives in north-western Alps: examples of earthquake-origin assessment of sedimentary disturbances. *Earth-Science Reviews* 96, 327–344.
- Begin, Z.B., Ehrlich, A., Nathan, Y., 1974. Lake Lisan, the Pleistocene precursor of the Dead Sea. *Geological Survey of Israel Bulletin* 63, 30.
- Begin, B.Z., Steinberg, D.M., Ichinose, G.A., Marco, S., 2005. A 40,000 years unchanging of the seismic regime in the Dead Sea rift. *Geology* 33, 257–260.
- Beinn, A., Amit, O., 1980. The evolution of the Dead Sea floating asphalt blocks: simulations by pyrolysis. *Journal of Petroleum Geology* 2, 439–447.
- Ben-Menahem, A., 1991. Four thousand years of seismicity along the Dead Sea rift. *Journal of Geophysical Research* 96 (B12), 20,195–20,216.
- Blay, P., Cosgrove, J.W., Summers, J.M., 1977. An experimental investigation of the development of structures in multilayers under the influence of gravity. *Journal of the Geological Society of London* 133, 329–342.
- Bookman (Ken-Tor), R., Enzel, Y., Agnon, A., Stein, M., 2004. Late Holocene lake levels of the Dead Sea. *Geological Society of America Bulletin* 116, 555–571.
- Bourgeois, J., Hansen, T.A., Wiberg, P.L., Kauffman, E.G., 1988. A tsunami deposit at the Cretaceous-tertiary boundary in Texas. *Science* 241, 567–570.
- Bradley, D., Hanson, L., 1998. Paleoslope analysis of slump folds in the Devonian flysch of Main. *Journal of Geology* 106, 305–318.
- Bryant, E., 2001. *Tsunami: the underrated hazard*. Cambridge University Press, Cambridge, UK 521 77599 X. 320 pp.
- Cita, M.B., Camerlenghi, A., Rimoldi, B., 1996. Deep-sea tsunami deposits in the eastern Mediterranean: new evidence and depositional models. *Sedimentary Geology* 104, 155–173.
- Collinson, J., 1994. Sedimentary deformational structures. In: Maltman, A.J. (Ed.), *The Geological Deformation of Sediments*. Chapman & Hall, London, pp. 95–125.
- Dasgupta, P., 2008. Experimental decipherment of the soft-sediment deformation observed in the upper part of the Talchir Formation (Lower Permian), Jharia Basin, India. *Sedimentary Geology* 205, 100–110.
- Dawson, A.G., Shi, S., 2000. Tsunami deposits. *Pure and Applied Geophysics* 157, 875–897.
- Dawson, A.G., Stewart, I., 2007. Tsunami deposits in the geological record. *Sedimentary Geology* 200, 166–183.
- Debacker, T.N., Sintubin, M., Verniers, J., 2001. Large-scale slumping deduced from structural and sedimentary features in the Lower Palaeozoic Anglo-Brabant fold belt, Belgium. *Journal of the Geological Society of London* 158, 341–352.
- Debacker, T.N., van Noorden, M., Sintubin, M., 2006. Distinguishing syn-cleavage folds from pre-cleavage folds to which cleavage is virtually axial planar: examples from the Cambrian core of the Lower Palaeozoic Anglo-Brabant Deformation Belt (Belgium). *Journal of Structural Geology* 28, 1123–1138.
- Debacker, T.N., Dumon, M., Matthys, A., 2009. Interpreting fold and fault geometries from within the lateral to oblique parts of slumps: a case study from the Anglo-Brabant Deformation Belt (Belgium). *Journal of Structural Geology* 31, 1525–1539.
- El-Isa, Z.H., Mustafa, H., 1986. Earthquake deformations in the Lisan deposits and seismotectonic implications. *Geophysical Journal of the Royal Astronomical Society* 86, 413–424.
- Elliot, C.G., Williams, P.F., 1988. Sediment slump structures: a review of diagnostic criteria and application to an example from Newfoundland. *Journal of Structural Geology* 10, 171–182.
- Farrell, S.G., 1984. A dislocation model applied to slump structures, Ainsa Basin, South Central Pyrenees. *Journal of Structural Geology* 6, 727–736.
- Farrell, S.G., Eaton, S., 1987. Slump strain in the Tertiary of Cyprus and the Spanish Pyrenees. Definition of palaeoslopes and models of soft sediment deformation. In: Jones, M.F., Preston, R.M.F. (Eds.), *Deformation of Sediments and Sedimentary Rocks: Special Publication of the Geological Society of London*, 29, pp. 181–196.
- Farrell, S.G., Eaton, S., 1988. Foliations developed during slump deformation of Miocene marine sediments, Cyprus. *Journal of Structural Geology* 10, 567–576.
- Fujiwara, O., Kamataki, T., 2008. Identification of tsunami deposits considering the tsunami waveform: an example of subaqueous tsunami deposits in Holocene shallow bay on southern Boso Peninsula, Central Japan. *Sedimentary Geology* 200, 292–313.
- Gardosh, M., Reches, Z., Garfunkel, Z., 1990. Holocene tectonic deformation along the western margin of the Dead Sea. *Tectonophysics* 180, 123–137.
- Garfunkel, Z., 1981. Internal structure of the Dead Sea leaky transform (rift) in relation to plate kinematics. *Tectonophysics* 80, 81–108.
- Haase-Schramm, A., Goldstein, S.L., Stein, M., 2004. U–Th dating of Lake Lisan aragonite (late Pleistocene Dead Sea) and implications for glacial East Mediterranean climate change. *Geochimica et Cosmochimica Acta* 68, 985–1005.
- Heifetz, E., Agnon, A., Marco, S., 2005. Soft sediment deformation by Kelvin Helmholtz instability: a case from Dead Sea earthquakes. *Earth and Planetary Science Letters* 236, 497–504.
- Holdsworth, R.E., 1988. The stereographic analysis of facing. *Journal of Structural Geology* 10, 219–223.

- Ichinose, G.A., Begin, Z.B., 2004. Simulation of tsunamis and lake seiches for the Late Pleistocene Lake Lisan and the Dead Sea. *Geological Survey of Israel Report GSI/7/04*, 50 pages.
- Ichinose, G.A., Anderson, J.G., Satake, K., Schweickert, R.A., Lahren, M.M., 2000. The potential hazard from tsunami and seiche waves generated by large earthquakes within Lake Tahoe, California–Nevada. *Geophysical Research Letters* 27, 1203–1206.
- Kagan, S., Stein, M., Agnon, A., Neumann, F., 2011. Intra-basin palaeoearthquake and quiescence correlation of the late Holocene Dead Sea. *Journal of Geophysical Research* 116, B04311. doi:10.1029/2010JB007452.
- Kastens, K.A., Cita, M.B., 1981. Tsunami-induced transport in the abyssal Mediterranean Sea. *Geological Society of America Bulletin* 92, 845–857.
- Ken-Tor, R., Agnon, A., Enzel, Y., Marco, S., Negendank, J.F.W., Stein, M., 2001. High-resolution geological record of historic earthquakes in the Dead Sea basin. *Journal of Geophysical Research* 106, 2221–2234.
- Kneller, B., 1995. Beyond the turbidite paradigm: physical models for deposition of turbidites and their implications for reservoir prediction. In: Hartley, A.J., Prosser, D.J. (Eds.), *Characterization of Deep Marine Clastic Systems*: Geological Society London Special Publication, 94, pp. 31–49.
- Lowe, D.J., de Lange, W.P., 2000. Volcano-meteorological tsunamis, the c.AD200 Taupo eruption (New Zealand) and the possibility of a global tsunami. *The Holocene* 401–407.
- Maltman, A., 1984. On the term soft-sediment deformation. *Journal of Structural Geology* 6, 589–592.
- Maltman, A., 1994a. *The Geological Deformation of Sediments*. Chapman & Hall, London, 362 pp.
- Maltman, A., 1994b. Introduction and overview. In: Maltman, A. (Ed.), *The Geological Deformation of Sediments*. Chapman & Hall, London, pp. 1–35.
- Marco, S., Agnon, A., 1995. Prehistoric earthquake deformations near Masada, Dead Sea graben. *Geology* 23, 695–698.
- Marco, S., Agnon, A., 2005. High-resolution stratigraphy reveals repeated earthquake faulting in the Masada Fault Zone, Dead Sea Transform. *Tectonophysics* 408, 101–112.
- Marco, S., Stein, M., Agnon, A., Ron, H., 1996. Long term earthquake clustering: a 50,000 year paleoseismic record in the Dead Sea Graben. *Journal of Geophysical Research* 101, 6179–6192.
- Marco, S., Weinberger, R., Agnon, A., 2002. Radial clastic dykes formed by a salt diapir in the Dead Sea Rift, Israel. *Terra Nova* 14, 288–294.
- Marco, S., Hartal, M., Hazan, N., Lev, L., Stein, M., 2003. Archaeology, history, and geology of the A.D. 749 earthquake, Dead Sea transform. *Geology* 31, 665–668.
- Martinsen, O.J., 1989. Styles of soft-sediment deformation on a Namurian delta slope, Western Irish Namurian Basin, Ireland. In: Whateley, M.K.G., Pickering, K.T. (Eds.), *Deltas: Sites and Traps for Fossil Fuels*: Geological Society of London Special Publication, 41, pp. 167–177.
- Martinsen, O.J., 1994. Mass movements. In: Maltman, A. (Ed.), *Mass Movements*. Chapman & Hall, London, pp. 127–165.
- Martinsen, O.J., 1994. Mass Movements. In: Maltman, A. (Ed.), *The Geological Deformation of Sediments*. Chapman & Hall, London, pp. 127–165.
- Martinsen, O.J., Bakken, B., 1990. Extensional and compressional zones in slumps and slides in the Namurian of County Claire, Eire. *Journal of the Geological Society of London* 147, 153–164.
- McHugh, C.M., Seeber, L., Braudy, N., Cormier, M.H., Davis, M.B., Diebold, J.B., Dieudonne, N., Douilly, R., Gulick, S.P.S., Hornbach, M.J., Johnson, H.E., Mishkin, K.R., Sorlien, C.C., Steckler, M.S., Symithe, S.J., Templeton, J., 2011. Offshore sedimentary effects of the 12 January 2010 Haiti earthquake. *Geology* 39, 723–726.
- Migowski, C., Agnon, A., Bookman, R., Negendank, J.F.W., Stein, M., 2004. Recurrence pattern of Holocene earthquakes along the Dead Sea transform revealed by varve-counting and radiocarbon dating of lacustrine sediments. *Earth and Planetary Science Letters* 222, 301–314.
- Moretti, M., Soria, J.M., Alfaro, P., Walsh, N., 2001. Asymmetrical soft-sediment deformation structures triggered by rapid sedimentation in turbiditic deposits (Late Miocene, Guadix Basin, southern Spain). *Facies* 44 (1), 283–294. doi:10.1007/BF02668179.
- Morton, R.A., Gelfenbaum, G., Jaffe, B.E., 2007. Physical criteria for distinguishing sandy tsunami and storm deposits using modern examples. *Sedimentary Geology* 200, 184–207.
- Mulder, T., 2011. Gravity processes and deposits on continental slope, rise and abyssal plains. In: Huneke, H., Mulder, T. (Eds.), *Deep-Sea Sediments. Developments in Sedimentology*, 63. Elsevier B.V., pp. 25–148, 750 pp.
- Nanayama, F., Shigeno, K., 2006. Inflow and outflow facies from the 1993 tsunami in southwest Hokkaido. *Sedimentary Geology* 187, 139–158.
- Nemer, T., Meghraoui, M., 2006. Evidence of coseismic ruptures along the Roum fault (Lebanon): a possible source for the AD 1837 earthquake. *Journal of Structural Geology* 28, 1483–1495.
- Nichols, G., 2009. *Sedimentology and Stratigraphy*, 2nd Edition. Wiley-Blackwell, 419 pages.
- Niemi, T.M., Ben-Avraham, Z., 1994. Evidence for Jericho earthquakes from slumped sediments of the Jordan River delta in the Dead Sea. *Geology* 22, 395–398.
- Nissenbaum, A., 1978. Dead Sea asphalts—historical aspects. *American Association of Petroleum Geologists Bulletin* 62, 837–844.
- Noda, A., Katayama, H., Sagatama, T., Suga, K., Uchida, Y., Satake, K., Abe, K., Okamura, Y., 2007. Evaluation of tsunami impacts on shallow marine sediments: an example from the tsunami caused by the 2003 Tokachi-oki earthquake, northern Japan. *Sedimentary Geology* 200, 314–327.
- Postma, G., Nemeč, W., Kleinspehn, K., 1988. Large floating clasts in turbidites: a mechanism for their emplacement. *Sedimentary Geology* 58, 47–61.
- Ramsay, J.G., 1967. *Folding and Fracturing of Rocks*. McGraw-Hill, New York, p. 555.
- Rodríguez-Pascua, M.A., De-Vicente, G., Calvo, J.P., Pérez-López, R., 2003. Similarities between recent seismic activity and paleoseismites during the late miocene in the external Betic Chain (Spain): relationship by 'b' value and the fractal dimension. *Journal of Structural Geology* 25, 749–763.
- Sarkar, S., Bose, P.K., Eriksson, P.G., 2011. Neoproterozoic tsunamiite: Upper Bhandar Sandstone, Central India. *Sedimentary Geology* 238, 181–190.
- Scheffers, A., Kelleter, D., 2003. Sedimentologic and geomorphologic tsunami imprints worldwide—a review. *Earth-Science Reviews* 63, 83–92.
- Shalem, N., 1956. Seismic tidal waves in the Eastern Mediterranean. *Society for Exploration of Israel*, v. 28, in Hebrew, pp. 159–170.
- Shapira, A., Avni, R., Nur, A., 1993. A note: new estimate of the Jericho earthquake epicentre of July 11, 1927. *Israel Journal of Earth Sciences* 42, 93–96.
- Strachan, L.J., 2008. Flow transformations in slumps: a case study from the Waitemata Basin, New Zealand. *Sedimentology* 55, 1311–1332.
- Strachan, L.J., Alsop, G.I., 2006. Slump folds as estimators of palaeoslope: a case study from the Fisherstreet Slump of County Clare, Ireland. *Basin Research* 18, 451–470.
- Sugawara, D., Minoura, K., Imamura, F., 2008. Tsunamis and tsunami sedimentology. In: Shiki, T., Tsuji, Y., Yamazaki, T., Minoura, K. (Eds.), *Tsunamiites—Features and Implications*. Elsevier B.V., pp. 9–49. doi:10.1016/B978-0-444-51552-0.00003-5. 411 pages.
- Wetzler, N., Marco, S., Heifetz, E., 2010. Quantitative analysis of seismogenic shear-induced turbulence in lake sediments. *Geology* 38, 303–306.
- Woodcock, N.H., 1976a. Ludlow Series slumps and turbidites and the form of the Montgomery Trough, Powys, Wales. *Proceedings of the Geologists Association* 87, 169–182.
- Woodcock, N.H., 1976b. Structural style in slump sheets: Ludlow Series, Powys, Wales. *Journal of the Geological Society of London* 132, 399–415.
- Woodcock, N.H., 1979. The use of slump structures as palaeoslope orientation estimators. *Sedimentology* 26, 83–99.